



저작자표시-비영리-변경금지 2.0 대한민국

이용자는 아래의 조건을 따르는 경우에 한하여 자유롭게

- 이 저작물을 복제, 배포, 전송, 전시, 공연 및 방송할 수 있습니다.

다음과 같은 조건을 따라야 합니다:



저작자표시. 귀하는 원저작자를 표시하여야 합니다.



비영리. 귀하는 이 저작물을 영리 목적으로 이용할 수 없습니다.



변경금지. 귀하는 이 저작물을 개작, 변형 또는 가공할 수 없습니다.

- 귀하는, 이 저작물의 재이용이나 배포의 경우, 이 저작물에 적용된 이용허락조건을 명확하게 나타내어야 합니다.
- 저작권자로부터 별도의 허가를 받으면 이러한 조건들은 적용되지 않습니다.

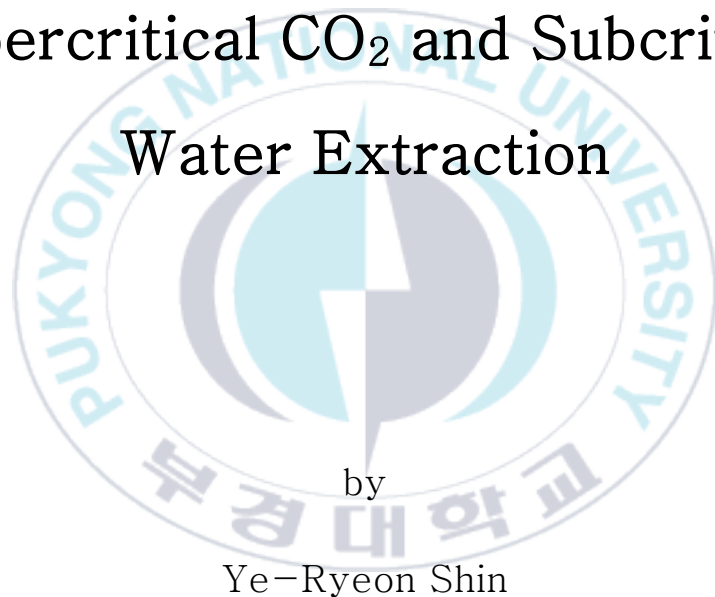
저작권법에 따른 이용자의 권리는 위의 내용에 의하여 영향을 받지 않습니다.

이것은 [이용허락규약\(Legal Code\)](#)을 이해하기 쉽게 요약한 것입니다.

[Disclaimer](#)

Thesis for the Degree of Master of Engineering

Valorization of Skipjack Tuna  
(*Katsuwonus pelamis*) By-products:  
Recovery of Lipids and Protein Using  
Supercritical CO<sub>2</sub> and Subcritical  
Water Extraction



by

Ye-Ryeon Shin

Department of Food Science and Technology

The Graduate School

Pukyong National University

February 2024

Valorization of Skipjack Tuna  
(*Katsuwonus pelamis*) By-products:  
Recovery of Lipids and Protein Using  
Supercritical CO<sub>2</sub> and Subcritical  
Water Extraction

가다랑어 (*Katsuwonus pelamis*) 부산물  
의 가치화: 초임계 이산화탄소와 아임계  
수 추출을 이용한 지질 및 단백질 회수

Advisor: Prof. Byung-Soo Chun

by

Ye-Ryeon Shin

A thesis submitted in partial fulfillment of the requirements  
for the degree of

Master of Engineering

in Department of Food Science and Technology, The Graduate School,  
Pukyong National University

February 2024

Valorization of Skipjack Tuna (*Katsuwonus pelamis*) By-products: Recovery of Lipids and Protein Using Supercritical CO<sub>2</sub> and Subcritical Water Extraction

A dissertation  
by  
Ye-Ryeon Shin

Approved by:

\_\_\_\_\_  
(Chairman)  
Ji-Yeong Yang, Ph.D.

\_\_\_\_\_  
(Member)  
Kil-Bo Shim, Ph.D.

\_\_\_\_\_  
(Member)  
Byung-Soo Chun, Ph.D.



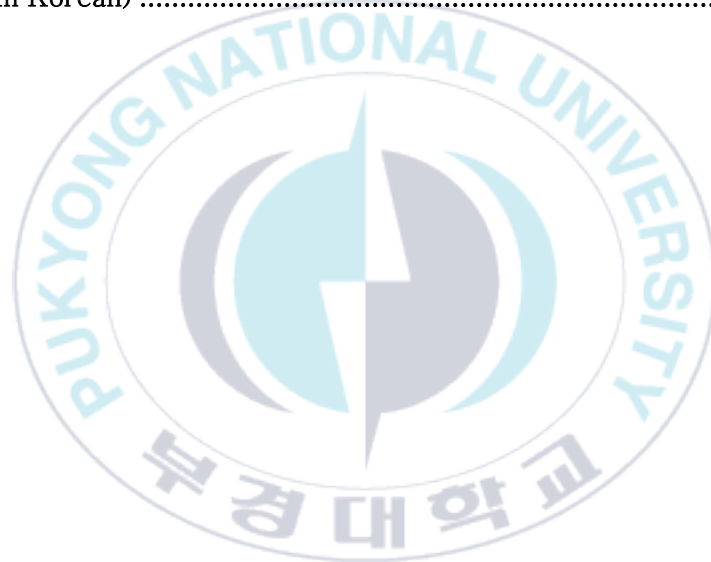
February 16, 2024

# Contents

List of Figures.....	iv
List of Tables.....	v
Abstract.....	vii
I . Introduction .....	1
II . Materials and methods .....	12
1. Materials and chemicals.....	12
2. Analysis of proximate compositions .....	12
3. Oil extraction using supercritical carbon dioxide (SC-CO <sub>2</sub> ) .....	13
4. Phospholipid extraction using SC-CO <sub>2</sub> with ethanol as co-solvent...	14
5. Lipids properties analysis.....	16
5.1. Measurement of lipid yield and purity .....	16
5.2. Phospholipids (PLs) quantification by <sup>31</sup> P NMR.....	17
5.3. Oil color analysis .....	17
5.4. Fatty acids composition analysis .....	18
5.5. Analysis of fat-soluble vitamins.....	20
5.6. Thermalgravimetric analysis (TGA) .....	22
6. Subcritical water hydrolysis (SWH) .....	22
7. Analysis of physicochemical properties of hydrolysate .....	25
7.1. Color analysis .....	25
7.2. pH analysis .....	25
7.3. Maillard reaction products (MRPs) measurements.....	25
7.4. Total sugar content measurements.....	26
7.5. Reducing sugar content measurements .....	26
7.6. Total protein content measurements.....	27

7.7. Sodium dodecyl sulfate–polyacrylamide gel electrophoresis (SDS–PAGE) analysis .....	27
7.8. Fourier transform infrared (FT–IR) spectrum analysis of hydrolysate .....	28
7.9. Amino acid analysis .....	28
7.9.1. Constituent amino acids analysis .....	29
7.9.2. Free amino acids analysis .....	29
8. Physiological activity of hydrolysate .....	30
8.1. Antioxidant activities of hydrolysate .....	30
8.1.1. DPPH radical scavenging activity .....	30
8.1.2. ABTS <sup>+</sup> radical scavenging activity .....	31
8.1.3. Ferric reducing antioxidant power (FRAP) .....	31
8.2. Antidiabetic activity .....	32
8.3. Anti–inflammatory activity .....	33
9. Statistical analysis .....	34
III. Result and Discussion .....	35
1. Proximate compositions of <i>K. pelamis</i> .....	35
2. Yield and purity of <i>K. pelamis</i> lipids .....	37
3. PLs composition of <i>K. pelamis</i> by <sup>31</sup> P NMR .....	42
4. Fatty acids composition of <i>K. pelamis</i> lipids .....	48
5. Fat–soluble vitamins of <i>K. pelamis</i> lipids .....	51
6. Thermogravimetric analysis (TGA) of <i>K. pelamis</i> lipids .....	53
7. Yield and MRPs of <i>K. pelamis</i> hydrolysate .....	57
8. pH and color of <i>K. pelamis</i> hydrolysate .....	60
9. Total sugar and reducing sugar in <i>K. pelamis</i> hydrolysate .....	64
10. Total protein content in <i>K. pelamis</i> hydrolysate .....	66
11. SDS–PAGE of <i>K. pelamis</i> hydrolysate .....	68
12. FT–IR spectrum of <i>K. pelamis</i> hydrolysate .....	71

13. Amino acid analysis of <i>K. pelamis</i> hydrolysate .....	75
14. Antioxidant activities of <i>K. pelamis</i> hydrolysate (DPPH, ABTS <sup>+</sup> , FRAP) .....	79
15. Antidiabetic activity of <i>K. pelamis</i> hydrolysate .....	82
16. Analysis of in vitro anti-inflammatory activity <i>K. pelamis</i> hydrolysate .....	85
IV. Conclusion.....	88
Reference.....	90
Abstract (In Korean) .....	101



## List of Figures

Figure 1. Body structure of Skipjack tuna ( <i>Katsuwonus pelamis</i> ) .....	5
Figure 2. Phase diagram of a substance with critical temperature and pressure .....	11
Figure 3. Schematic diagram of the SC-CO <sub>2</sub> extraction.....	15
Figure 4. Schematic diagram of the subcritical water hydrolysis apparatus.....	24
Figure 5. Visual appearance of extracted oils from <i>K. pelamis</i> .....	41
Figure 6. <sup>31</sup> P NMR spectra of phospholipid extracted from different parts of <i>K. pelamis</i> .....	46
Figure 7. TGA (Thermogravimetric Analysis) of lipids extracted from different parts of <i>K. pelamis</i> .....	56
Figure 8. Visual appearance of SWE hydrolysates from different parts of <i>K. pelamis</i> .....	63
Figure 9. SDS-PAGE pattern of SWE hydrolysates from different conditions of <i>K. pelamis</i> .....	70
Figure 10. Infrared absorption properties of <i>K. pelamis</i> by FT-IR analysis.....	74

## List of Tables

Table 1. Scientific Classification.....	4
Table 2. Critical properties of various solvents (Cansell et al., 1999) .....	10
Table 3. Gas chromatography operating conditions for fatty acid analysis.....	19
Table 4. Analytical conditions of vitamin A, E by HPLC .....	21
Table 5. Proximate compositions of <i>K. pelamis</i> by-products.....	36
Table 6. Yield, purity content of lipid extracted from <i>K. pelamis</i> .....	39
Table 7. Color properties of oils extracted from <i>K. pelamis</i> .....	40
Table 8. Phospholipid composition ( $\mu$ mol/g oil, %) of <i>K. pelamis</i> determined by $^{31}\text{P}$ NMR.....	47
Table 9. Fatty acid composition <i>K. pelamis</i> oil .....	49
Table 10. Fatty acid composition <i>K. pelamis</i> phospholipid.....	50
Table 11. Fat-soluble vitamin contents of lipids extracted from different parts of <i>K. pelamis</i> .....	52
Table 12. Yield of SWE hydrolysates from different parts of <i>K. pelamis</i> .....	58
Table 13. Maillard reaction products (MRPs) of SWE hydrolysates from different parts of <i>K. pelamis</i> .....	59
Table 14. pH properties of SWE hydrolysates from different parts of <i>K. pelamis</i> .....	61

Table 15. Color properties of SWE hydrolysates from different parts of <i>K. pelamis</i> .....	62
Table 16. Total sugar & reducing sugar contents of SWE hydrolysates from different parts of <i>K. pelamis</i> .....	65
Table 17. Total protein contents of SWE hydrolysates from different parts of <i>K. pelamis</i> .....	67
Table 18. Constituent amino acids profiles of SWE hydrolysates from different parts of <i>K. pelamis</i> .....	77
Table 19. Free amino acids profiles of SWE hydrolysates from different parts of <i>K. pelamis</i> .....	78
Table 20. Antioxidant activities of SWE hydrolysates from different parts of <i>K. pelamis</i> .....	81
Table 21. $\alpha$ -Glucosidase inhibitory activity of <i>K. pelamis</i> de-oiled hydrolysates obtained at different conditions.....	83
Table 22. IC <sub>50</sub> values of $\alpha$ -glucosidase inhibitory activity of <i>K. pelamis</i> hydrolysate extracted at 240 °C. ....	84
Table 23. Analysis of protein denaturation inhibition of <i>K. pelamis</i> de-oiled hydrolysates obtained at different conditions. ....	87

# Valorization of Skipjack Tuna (*Katsuwonus pelamis*) By-products: Recovery of Lipids and Protein Using Supercritical CO<sub>2</sub> and Subcritical Water Extraction

Ye-Ryeon Shin

Department of Food Science and Technology, The Graduate School,  
Pukyong National University

## Abstract

Skipjack tuna (*Katsuwonus pelamis*) serves as the primary raw material for processed fishery products. By-products produced during fishing and processing make up roughly 50% of the raw material. However, the disposal and processing of these by-products can lead to adverse environmental impacts. Therefore, this study aimed to extract lipids and proteins from skipjack tuna by-products (including the head, viscera, and skin) using innovative and environmentally friendly methods of supercritical carbon dioxide and subcritical water. Oil was extracted utilizing supercritical carbon dioxide with fixed conditions of 55°C temperature and 30 MPa pressure. Phospholipids were then continuously extracted using degreased powder and a co-solvent of ethanol and supercritical carbon dioxide, at a temperature of 40°C, a pressure of 30 MPa, a carbon dioxide flow rate of 6 mL/min, and a co-solvent flow rate of 10% of the carbon dioxide flow rate. The protein was recovered from de-oiled powder using subcritical water hydrolysis, and then extracted and compared at a temperature between 160 and 240°C. The pressure was maintained at 3 MPa for 15 min with a ratio of 1:50 (w/v). The skin oil (SO) extracted from skipjack tuna had the highest oil yield at 31.18% ± 0.59%. In contrast, the head oil (HO) and viscera oil (VO) resulted in 14.20% ± 0.67% and 13.79% ± 1.05% oil, respectively. Phospholipid yields varied by body part, with the head yielding the highest net phospholipid content at 3.24%, 2.47%, and 1.68%, respectively. A qualitative and quantitative analysis was conducted using the <sup>31</sup>P NMR spectrum of phospholipids. The major classes identified were phosphatidylcholine (PC), phosphatidylethanolamine (PE), and lysophosphatidylcholine (LPC), with PC accounting for more than 70% of the major classes. Palmitic acid, oleic acid, and docosahexaenoic acid (DHA) have been identified as the primary fatty acids found in lipids. These fatty acids account for 28.26%, 15.74%, and 30.02% of ω-3 in oil and 7.89%, 15.82%, and 19.91% of phospholipids, respectively. Additionally, the sample contained fatty acids. Retinol was detected at 1.06 ± 0.02 mg/100g solely in the viscera oil, while tocopherol, a major vitamin, was found in both the oil and phospholipids. In the oil,

$\gamma$ -tocopherol measured  $29.73 \pm 0.13$  mg/100g,  $17.88 \pm 0.02$  mg/100g, and  $76.57 \pm 0.84$  mg/100g, and in the phospholipids, it was  $25.98 \pm 0.12$  mg/100g,  $18.90 \pm 0.11$  mg/100g, and  $19.49 \pm 0.09$  mg/100g. Additionally, thermogravimetric analysis indicated that the oil exhibited excellent thermal stability, as it experienced simple weight reduction. The extraction yield of skipjack tuna hydrolysate increased as the temperature rose, with the highest yield obtained in the viscera hydrolysate (VH) at  $90.17\% \pm 0.96\%$ . The production of Maillard reactants increased with the increasing temperature, as confirmed through the Maillard reaction products (MRPs) results. The study indicates that as temperature increased, the total sugar content generally decreased. The sugar content varied between  $6.44 \pm 0.22$  to  $13.34 \pm 0.67$  mg glucose/g dried sample,  $12.81 \pm 0.20$  to  $55.19 \pm 0.82$  mg glucose/g dried sample, and  $6.34 \pm 0.11$  to  $13.69 \pm 0.49$  mg glucose/g dried sample. The highest reducing sugar content was observed at  $200^\circ\text{C}$  for the head hydrolysate (HH), with  $8.87 \pm 1.09$  mg glucose/g dried sample, at  $220^\circ\text{C}$  with  $23.62 \pm 2.04$  mg glucose/g dried sample, and for the extract of the VH and SH with  $7.95 \pm 0.43$  mg glucose/g dried sample. The content decreased as the temperature increased. SDS-PAGE confirmed that the molecular weights of 75 KDa, 63 KDa, and 35 KDa were mainly reduced to low molecular weight compounds above  $200^\circ\text{C}$  at each parts. The total protein content in all parts exhibited a decreasing trend, with the highest values observed at  $200^\circ\text{C}$  ( $219.86 \pm 2.26$  mg BSA/g dried sample,  $297.36 \pm 2.17$  mg BSA/g dried sample, and  $265.88 \pm 0.85$  mg BSA/g dried sample). Upon analysis of the amino acid composition of the  $200^\circ\text{C}$  hydrolysates with the highest protein content, the primary constituent amino acids were found to be leucine, glutamic acid, glycine, arginine, and alanine. Additionally, histidine and taurine were marked as the main free amino acids. A variance in content was observed in comparison to raw sample. The antioxidant activity of the hydrolysate increased with temperature, reaching its highest levels at  $240^\circ\text{C}$ , specifically at  $52.21 \pm 1.05$  mg Trolox/g dried sample,  $80.30 \pm 1.70$  mg Trolox/g dried sample, and  $68.28 \pm 7.19$  mg Trolox/g dried sample. Progressively higher antidiabetic activity also occurred as the temperature increased. The  $\text{IC}_{50}$  values for  $\alpha$ -glucosidase inhibition were  $6.38 \pm 0.09$  mg/ml,  $2.08 \pm 0.17$  mg/ml, and  $5.18 \pm 0.14$  mg/ml at  $240^\circ\text{C}$ , respectively. The VH displayed the highest level of activity when contrasted with extracts from other parts. Anti-inflammatory activity also showed maximum activity at  $240^\circ\text{C}$ , and the highest activity was shown in the VH. Based on the study findings, skipjack tuna is deemed a viable raw material for both the food and pharmaceutical industries. Supercritical carbon dioxide and subcritical water extraction techniques were identified as critical data that will enable researchers and industry experts to selectively use it in future studies. It is highly likely that the use of skipjack tuna will continue to expand in these fields.

## I . Introduction

Skipjack tuna (*Katsuwonus pelamis*) is a species belonging to the mackerel family. The scientific classification of skipjack tuna is shown in Table 1. As shown in Figure 1, It is characterized by its long, cylindrical body, with scales primarily found on the chest and lateral lines. The dorsal side exhibits a deep blue color, while the ventral side is silver in appearance. This species features 4 to 6 dark bands run longitudinally on its body, appearing as disjointed dark spots when alive (Collette & Nauen, 1983). Spawning of skipjack tuna occurs throughout the year in equatorial waters, whereas in subtropical regions, it predominantly takes place from spring to early fall, with the duration of the spawning season decreasing as one moves away from the equator (Matsumoto et al., 1984). Fertility in skipjack tuna is size dependent, with the number of eggs per season ranging from 80,000 to 2 million for females measuring between 41 to 87 cm in length. This species primarily feeds on a variety of fish species, crustaceans, and mollusks. Skipjack tuna is well-known for its pelagic nature and extensive migratory patterns. It is commonly found in tropical and subtropical waters across all the world's oceans, with a significant catch occurring in the western North Pacific, particularly in the Pacific (Mugo et al., 2010). According to data from the National Statistical Office, skipjack tuna production has exhibited fluctuations over the years, increasing from 173,333 metric tons in 2011 to 290,302 metric tons in 2019, but subsequently declining to 202,303 metric tons in 2022. Domestic import and export volumes of skipjack tuna remained relatively stable, ranging from 160,336 (M/T) in 2011 to 169,468 (M/T) in 2019. However,

there was a significant decrease to 100,040 (M/T) in 2022 (MOF, 2022). Skipjack tuna is predominantly processed into bonito flakes known as katsuobushi, which are widely used in soup dishes and canned products. Skipjack tuna contributes to more than 55% of all canned fish products (Kenneth, 2010). Nevertheless, a significant portion of skipjack tuna by-products, including fish bones, heads, scales, viscera, and skin, have traditionally been processed into low-value fishmeal for animal feed or treated as waste (Zhang et al., 2019). However, there is a growing interest in extracting and utilizing valuable nutrients from these by-products, such as fish oil, protein, collagen, gelatin, and enzymes. Furthermore, attention is now being directed towards the environmental impact of the underutilization and disposal of substantial by-product quantities, making research in this area increasingly significant.

The research on skipjack tuna by-products has encompassed a variety of investigations, including the purification and characterization of trypsin from skipjack tuna spleen (Klomklao et al., 2007), enzymatic hydrolysis of skipjack tuna viscera (Klomklao & Benjakul, 2017), isolation of gelatin from skipjack tuna skin, and the characterization of acid and pepsin soluble collagen from the spine and skull of skipjack tuna (Shyni et al., 2014). Additionally, studies have focused on oil extraction from skipjack tuna eyeballs using wet rendering (Puttikajorn & Benjakul, 2020), purification and characterization of lectins from skipjack tuna eggs (Jung et al., 2003), evaluation of the antibacterial function of antimicrobial peptides isolated from skipjack tuna liver (Seo et al., 2014), and the analysis of antioxidant peptides obtained from hydrolysates of skipjack tuna protein (Wang et al., 2022), among others. Fish is recognized as a valuable source of various functional biomateri-

als, including polyunsaturated fatty acids (PUFA), polysaccharides, phospholipids, minerals, vitamins, antioxidants, enzymes, and bioactive peptides. Proteins, in particular, assume a pivotal role and have garnered significant interest due to the potential of protein hydrolysates in enhancing the functional attributes of natural proteins. These hydrolysates have found applications in cosmetics, medicine, food, and nutrition (Villamil et al., 2017). Marine by-products, such as skin, intestines, and blood resulting from marine processing, contain significant protein content and offer a promising source of bioactive peptides. The biological activity of these peptides is closely linked to their amino acid composition and sequence. Numerous fish species, including smelt, herring, yellowfin tuna, salmon, grass carp, white lotus, flounder, snakehead, mackerel, pollack, and tilapia, have been shown to possess notable biological activities, such as antioxidant, antihypertensive, immunomodulatory, and antibacterial properties, as demonstrated in multiple studies (Abuine et al., 2019; Chalamaiah et al., 2012).

Table 1. Scientific Classification

Scientific Classification	
Kingdom	Animalia
Phylum	Chordata
Class	Actinopterygii
Order	Scombriformes
Family	Scombridae
Genus	<i>Katsuwonus</i>
Species	<i>K. pelamis</i>



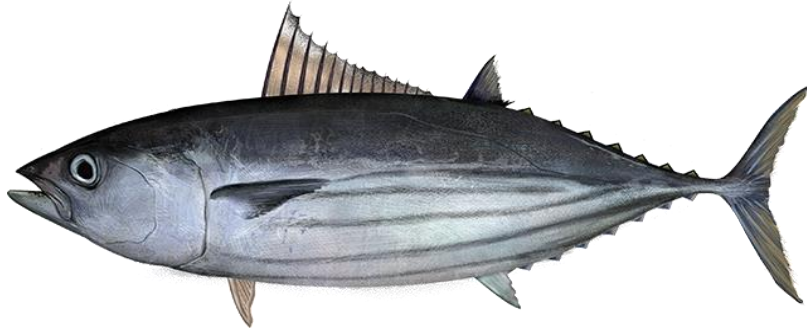


Figure 1. Body structure of Skipjack tuna (*Katsuwonus pelamis*).



The health benefits associated with fish consumption are primarily attributed to its abundant protein content, essential unsaturated fatty acids, minerals, and vitamins. Notably, fish oil, rich in polyunsaturated fatty acids (PUFA), particularly  $\omega$ -3 PUFA, has drawn significant attention. Skipjack tuna is recognized for its high levels of  $\omega$ -3 fatty acids, such as Docosahexaenoic acid (DHA) or Eicosapentaenoic acid (EPA). Over the past few decades, the pharmaceutical and food industries have shown a growing interest in the potential advantages of DHA and EPA intake (García-Moreno et al., 2014). These fatty acids are known to promote cardiovascular health and alleviate inflammatory conditions like asthma, eczema, and Crohn's disease (Pike & Jackson, 2010).

Phospholipids (PLs) are essential amphipathic compounds characterized by a hydrophilic head and a hydrophobic tail. They serve as critical components of cell membranes and, due to their unique emulsifying properties and physicochemical characteristics, are widely utilized as effective dispersants, stabilizers, or emulsifiers in the food, cosmetics, and pharmaceutical industries (Haq et al., 2021). The most common PLs structures involve those with a glycerol backbone, sphingomyelin, and alkoxy glycerol based PLs with a fatty chain linked by an ether bond at the sn-1 position of the glycerol skeleton. Glycerol PLs exhibit a shared structure consisting of two fatty acid (FA) molecules esterified at the sn-1 and sn-2 positions of the glycerol moiety, forming a hydrophobic segment. The sn-3 position of a glycerophospholipid molecule contains a phosphate group bound to a hydrophilic residue, contributing to the molecule's overall hydrophilicity (Lordan et al., 2017). The major PLs, including phosphatidylcholine (PC), phosphati-

dylethanolamine (PE), phosphatidylinositol (PI), and phosphatidylserine (PS), are identified based on this sn-3 position. Marine phospholipids (MPLs) primarily consist of PLs containing DHA or EPA and are gaining significance in food industry research (Hamadou et al., 2020). MPLs readily integrate into cell membranes and plasma lipoproteins, including high-density lipoprotein (HDL). Consequently, they not only exhibit superior bioavailability of  $\omega$ -3 polyunsaturated fatty acids but are also associated with a range of health benefits, such as the relief of symptoms related to rheumatoid arthritis and the reduction of the risks of developing cardiovascular, central nervous system, cancer, diabetes, and coronary heart diseases (Lordan et al., 2020).

Supercritical fluid (SCF) is a unique substance that exhibits distinct properties when subjected to temperatures and pressures exceeding its critical point. At such conditions, SCF displays characteristics that fall between those of gases and liquids, with lower density and viscosity compared to traditional liquids, and diffusion properties similar to gases. One of the major advantages of SCF is its ability to extract organic compounds from matrices without relying on conventional organic solvents, making it a cost-effective and safe alternative for extraction. The commercial use of SCF was initially observed in applications such as hop extraction and coffee decaffeination. It is primarily employed in the extraction of natural products like essential oils and lipid products and can also be used for concentration purposes (Clifford & Williams, 2000). As can be compared through the critical conditions for various solvents in Table 2, carbon dioxide (CO<sub>2</sub>) is the most commonly utilized fluid for supercritical fluid extraction, mainly due to its lower critical conditions (31 °C and 7.4 MPa) compared to other fluids (Table 2). Supercritical carbon dioxide (SC-CO<sub>2</sub>) offers numerous ecological and

practical advantages over traditional extraction methods (Haq et al., 2021). Because it doesn't require high temperatures during the extraction process, SC-CO<sub>2</sub> is well suited for obtaining high-quality oil from fish by-products while minimizing the oxidation of  $\omega$ -3 fatty acids (Franklin et al., 2020). In addition, it is colorless, non-toxic, non-flammable, excellent in recovering samples at low cost, has no residual solvent after extraction, and is a process with excellent stability and economic efficiency with the advantage of being able to reuse CO<sub>2</sub> (Jeong et al., 2021; Turner et al., 2001). SC-CO<sub>2</sub> can also be applied to extract PLs. Traditionally, PLs have been extracted using organic solvents like ethanol, dimethyl ether, chloroform, and hexane, which can have adverse effects on the environment and consumer health (Haq et al., 2018). However, as PLs are protic substances, effective extraction with CO<sub>2</sub> alone can be challenging. To address this issue, PLs can be recovered by introducing a polar cosolvent into SC-CO<sub>2</sub>, improving density, diffusivity, viscosity, and solubility. This, in turn, reduces interfacial tension and viscosity, enhancing the mass transfer rate (Jessop & Subramaniam, 2007). When considering food safety and consumer health when selecting a co-solvent, ethanol can be used as a suitable alternative to meet these conditions, so ethanol was used as a co-solvent in this study.

Subcritical water extraction (SWE) involves using water as a solvent within a temperature range between the boiling point at 1 bar (100°C) and the critical point at 220 bar (374°C). The phase diagram of a substance with critical temperature and critical pressure is shown in Figure 2. This process is considered eco-friendly because it enables the extraction of a variety of bioactive compounds without compromising the quality of the extract (Chun et al., 2022). In the subcritical state, water

exhibits unique properties, including an increase in ionic products, three times higher than those under environmental conditions, resulting in changes in the hydrogen bond structure. This increase in ionic products facilitates the formation of hydronium ( $\text{H}_3\text{O}^+$ ) and hydroxide ( $\text{OH}^-$ ) ions, making it suitable for recovering various bioactive materials, such as proteins (Chang et al., 2022; Haque et al., 2023). Additionally, it can dissolve organic substances that are typically insoluble in regular water, allowing the extraction of valuable substances and reducing their molecular weight. As water is a safe solvent, there is no need to remove it from the final product, making it a viable alternative to traditional solvent-based extraction methods.

Therefore, the study attempted to utilize sustainable and eco-friendly processes of subcritical water and supercritical carbon dioxide extraction to obtain valuable compounds such as lipids and amino acids from the by-products of skipjack tuna. The results of this research are expected to provide valid data to the food and pharmaceutical industries by indicating the potential to enhance the added value of skipjack tuna by-products.

Table 2. Critical properties of various solvents (Cansell et al., 1999)

Fluid	Critical temperature (°C)	Critical pressure (MPa)	Critical density (g/cm <sup>3</sup> )
Carbon dioxide	31.2	7.38	468
Ammonia	132.4	11.29	235
Water	374.1	22.10	317
Ethylene	9.5	5.06	220
Ethane	32.5	4.91	212
Propane	96.8	4.26	225
n-Pentane	196.6	3.37	232
Cyclohexane	279.9	4.03	270
Methanol	240.0	7.95	275
Ethanol	243.1	6.39	280
Isopropanol	235.6	5.37	274
Acetone	235.0	4.76	273

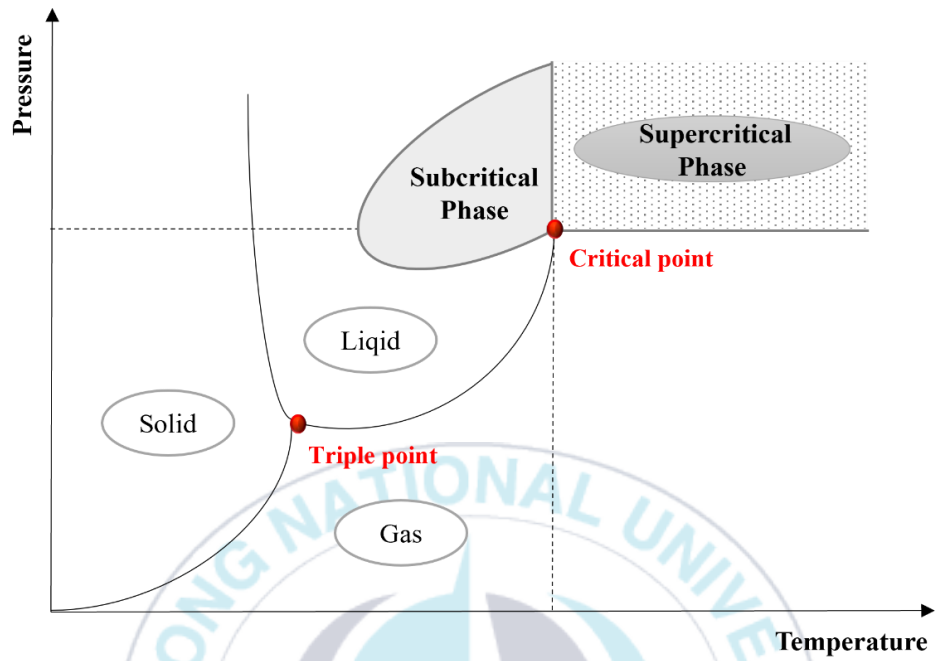


Figure 2. Phase diagram of a substance with critical temperature and pressure.

## II. Materials and methods

### 1. Materials and chemicals

Dongwon Fisheries Co. Ltd, located in Busan, South Korea, generously supplied skipjack tuna samples. These samples were categorized into different parts including the head, viscera, and skin. Subsequently, they were freeze-dried, stored at  $-40^{\circ}\text{C}$ , and blended using a blender. Food grade carbon dioxide (99.5% pure) and nitrogen gas were purchased from KOSEM (Saha-gu, Korea). All other reagents and standards were analytical or high-performance liquid chromatography (HPLC) grade.

### 2. Analysis of proximate compositions

Proximate composition analysis was conducted on skipjack tuna by-products using the AOAC official methods in accordance with our prior study. The carbohydrate content was calculated by subtracting the remaining constituents (moisture, crude fat, crude protein, and ash) from the total content of 100%.

To determine moisture content, 3 g of the powdered sample were placed in a weighing dish with a known constant weight and dried at  $100^{\circ}\text{C}$  until a consistent weight was achieved.

Crude fat analysis was carried out using a Soxhlet extractor, where 5 g of the powdered sample were covered with cotton wool using a cylindrical filter paper. Lipids were extracted at  $85^{\circ}\text{C}$  for 30 h with 100

mL of n-hexane. The n-hexane was subsequently removed at 45 °C using a rotary evaporator (Eyela N-1100, Rikakikai, China), and the crude lipid content was determined.

For the analysis of crude protein, the micro-Kjeldahl method was employed. This involved combining 20 mL of sulfuric acid and a decomposition accelerator ( $\text{CuSO}_4:\text{K}_2\text{SO}_4$ , 1:4) in a Kjeldahl flask with 1 g of the powdered sample. A Kjeldahl decomposition device (Digestion Unit K-425, BUCHI, Switzerland) was used for this purpose. The nitrogen content was determined by multiplying the sample weight by the nitrogen conversion factor (6.25).

The ash content was determined by heating 1 g of the powdered sample in a pre-weighed crucible in a muffle furnace at 550 °C until an off-white ash was obtained.

### 3. Oil extraction using supercritical carbon dioxide (SC-CO<sub>2</sub>)

Oil extraction from freeze-dried raw sample using supercritical carbon dioxide (SC-CO<sub>2</sub>) extraction equipment. The system was equipped with a carbon dioxide (CO<sub>2</sub>) pump, a cooler for liquefaction, a heat exchanger for temperature control, a separator, a back pressure regulator (BPR) valve, and a needle valve. The extraction parameters, based on the optimal conditions as determined by Park et al. (2022), were set at a temperature of 55 °C and a pressure of 30 MPa. To prevent sample leakage, 50 g of freeze-dried sample was placed inside the 200 cm<sup>3</sup> extraction vessel. To prevent sample leakage, defatted filter papers were positioned above and below the sample, and the vessel was sealed.

CO<sub>2</sub> gas was then injected to reach the desired pressure, initiating the extraction process. The flow rate of CO<sub>2</sub> was maintained at a constant 27 g/min, and the extraction procedure lasted for a duration of 2 h. The extracted oil was subsequently stored in a dark environment at -40°C until it was utilized in the subsequent analyses.

#### 4. Phospholipid extraction using SC-CO<sub>2</sub> with ethanol as co-solvent

The de-oiled skipjack tuna (DST) powder obtained from the laboratory-scale SC-CO<sub>2</sub> extraction was used for phospholipid (PLs) extraction using the same extraction system with ethanol as co-solvent. A schematic diagram of the extraction system is shown in Figure 3. The system was equipped with a CO<sub>2</sub> pump, an ethanol delivery pump and column oven, as well as a back pressure regulator. The extraction conditions comprised a temperature of 40°C, a pressure of 30 MPa, an SC-CO<sub>2</sub> flow rate of 6 mL/min, and a co-solvent flow rate equivalent to 10% of the SC-CO<sub>2</sub> flow rate, with a fixed extraction duration of 2 h. The ethanol-PLs mixture underwent ethanol evaporation using a nitrogen concentrator (NDK200-2N, Hangzhou Miu Instruments Co., Ltd., China). The resulting sample was stored in a dark environment at -40°C until further analysis.

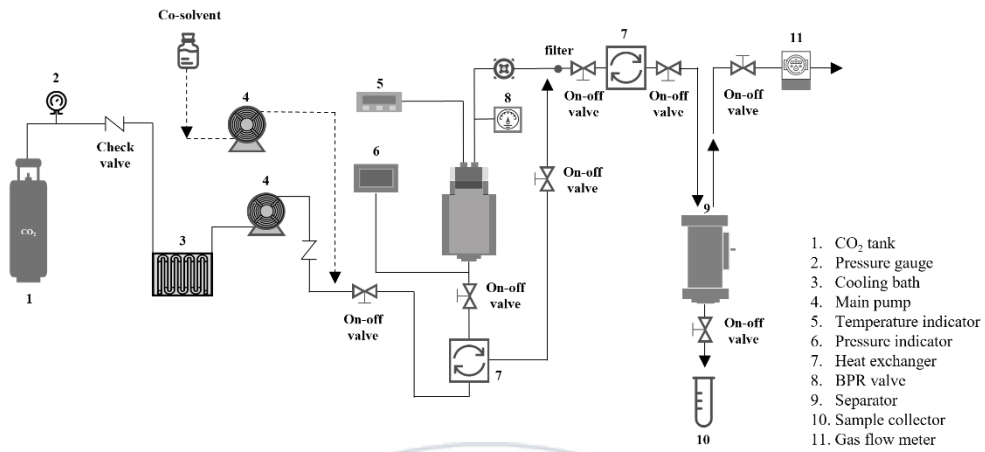
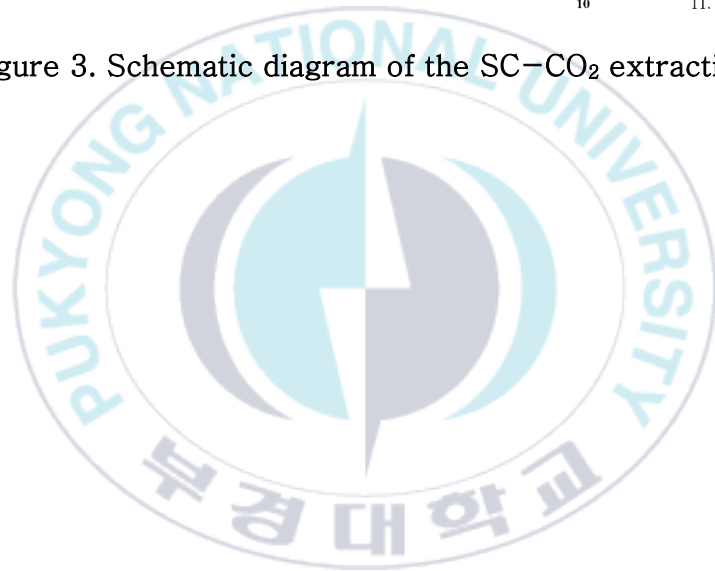


Figure 3. Schematic diagram of the SC-CO<sub>2</sub> extraction.



## 5. Lipids properties analysis

### 5.1. Measurement of lipid yield and purity

The percentage of obtained from DST samples was used to express the yield of PLs. To evaluate the purity of the PLs, a colorimetric method by Stewart J. C. M. (1980) was employed. For sample preparation, 10 mg of the extracted PLs from skipjack tuna were dissolved in 1 mL of chloroform. Subsequently, 100  $\mu$ L of the sample solution, 800  $\mu$ L of chloroform, and 100  $\mu$ L of a mixed solution containing ferric chloride (27 g/L) and ammonium thiocyanate (30 g/L) (in a 1:1, v/v ratio) were added to a 2 mL microcentrifuge tube. The tube contents were thoroughly mixed for 1 min. The tube was then centrifuged in a microcentrifuge (MAXpin C12–mt, DAIHAN Scientific Co. Ltd., Korea) at 10,000 g for 15 min, and the lower phase was carefully transferred to a UV/Vis glass cuvette. The absorbance was measured at 488 nm using a Shimadzu UV mini-1240 spectrophotometer in Kyoto, Japan. The PC standard curve was generated by utilizing a commercial PC standard (Sigma–Aldrich Inc. located in St. Louis, MO, USA), which was set to a concentration range of 0–1 mg/mL. The net PLs content of the extracted lipids was calculated using the following equation, which was adapted from the work of Haq M. (2018) (Haq et al., 2018).

$$PL \text{ yield (\%)} = \frac{(\text{Amount of PL in the polar lipids})}{(\text{Dried biomass})} \times 100$$

## 5.2. Phospholipids (PLs) quantification by $^{31}\text{P}$ NMR

Qualitative and quantitative analysis of each PLs region extracted through SC-CO<sub>2</sub> was conducted via phosphorus-31 nuclear magnetic resonance ( $^{31}\text{P}$  NMR) analysis using the JNM ECZ-400 MHz instrument from JEOL, Ltd., based in Tokyo, Japan. Commercial soybeans and egg yolk lecithin served as standard materials. The methodology was adapted from Yao L. (2010) with some modifications (Yao & Jung, 2010). To prepare the samples, a solution of Cs-EDTA (0.2 N, pH 8.5) was obtained by adjusting the pH to 8.5 using CsOH in 0.2 N EDTA. Approximately 80–90 mg of the sample and 5 mg of triphenyl phosphate (TPP) were added. In addition, 1 mL each of chloroform-d, methanol, and Cs-EDTA (0.2 N, pH 8.5) were included. The mixture was vigorously stirred, and the lower phase was passed through a 0.20  $\mu\text{m}$  hydrophilic syringe filter after filtration. Once filtered, it was transferred to a 5 mm NMR tube. The NMR acquisition parameters were set to Scans = 400, sweep width = 6500 Hz, relaxation delay = 10 s, excitation pulse = 45°, temperature = 25 °C, and data points=32,768. The TPP had a chemical shift of -17.8 ppm, and each PL compound was referenced to it. Individual quantification of PL was performed using JEOL Delta version 6.2.0 (JEOL, Ltd., Tokyo, Japan) based on the following equation.

$$\text{Phospholipid (PL)} = \text{Integral} \times \frac{\text{number of phosphorus (TPP)}}{\text{Number of phosphorus (PL)}} \times \text{Conc. (TPP)}$$

## 5.3. Oil color analysis

The color of lipids extracted using SC-CO<sub>2</sub> was assessed using a colorimeter (Lovibond RT series, The Tintometer Ltd, Amesbury, UK). The results were expressed in the form of three-dimensional coordinate values consisting of L\*, a\*, and b\*. L\* indicates brightness (ranging from 0 to 100), a\* indicates the extent of redness (+a\*) and greenness (-a\*), and b\* indicates the degree of yellowness (+b\*) and blueness (-b\*). The standard plate values were the following: L\* = 94.61, a\* = -1.03, and b\* = -0.20.

#### 5.4. Fatty acids composition analysis

The lipids obtained through SC-CO<sub>2</sub> extraction were subjected to analysis using a Gas Chromatography (GC) device (6890N, Agilent Technologies, Inc., CA, USA). Fatty acid methyl esterification (FAME) was performed in accordance with the AOCS official method Ce 2-66 (1998) (AOCS, 1998). The sample were mixed with 2 mL of a 0.1% hexane solution containing C<sub>17</sub> (heptadecanoic acid) and 3 mL of 0.5 N NaOH methanol solution. The mixture was stirred and then heated to 75°C for 45 min. After cooling at room temperature for 10 min, 3 mL of boron trifluoride (BF<sub>3</sub>) were added. The mixture heated to 75°C for an additional 20 min. It was cooled once more at room temperature for 10 min. A further 3 mL of hexane for HPLC and 1 mL of 10% NaCl were added. The supernatant was then filtered using a 0.20 μm hydrophobic syringe filter. GC operating conditions are shown in Table 3.

Table 3. Gas chromatography operating conditions for fatty acid analysis

Parameter	Conditions
Instrument	Agilent 6890N GC System
Split	Splitless
Inject Temperature	250°C
Carrier Gas & Flow Rate	He, 0.5 mL/min
Oven Condition	140°C (5 min) → 4°C/min for 25 min → 240°C (17 min)
Detect Temperature	260°C
Column	Supelco sp. 2560, capillary column Fused silica Capillary 100 m × 250 μm × 0.2 μm film thickness

## 5.5. Analysis of fat-soluble vitamins

The fat-soluble vitamins extracted from lipids using SC-CO<sub>2</sub> were subjected to analysis via HPLC, with modifications based on the method by Park J. S. (2022) (Park et al., 2022). Specifically, Vitamins A (Retinol) and E (Tocopherol) were the focus of analysis. The procedure involved mixing 1 g of lipid with 1 mL of a 10% pyrogallol-ethanol solution and 3 mL of a 90% potassium hydroxide solution. The flask was then partially immersed in a 95°C water bath, with a reflux condenser employed for saponification over a period of 30 min. Following the reaction, the mixture was rapidly cooled to room temperature. The petroleum ether layer was separated by washing with a mixture of distilled water and petroleum ether, followed by a wash with sodium sulfate. The petroleum ether layer was subsequently evaporated using a nitrogen concentrator. The resulting dried product was dissolved in chloroform, diluted with propanol, and filtered through a 0.45 μm syringe filter before analysis. HPLC conditions for each vitamin are detailed in Table 4.

Table 4. Analytical conditions of vitamin A, E by HPLC

Parameters	Vitamin A & E
Wavelength	298 nm
Oven temperature	30°C
Mobile phase	MeOH : Water (95 : 5, v/v)
Flow rate	0.5 mL/min
Column	YMC Carotenoid 5 $\mu$ m C <sub>30</sub> (4.6x250 mm)
Injection volume	10 $\mu$ L

## 5.6. Thermalgravimetric analysis (TGA)

TGA of lipids extracted by SC-CO<sub>2</sub> was conducted using a thermo-gravimetric analyzer (Discovery TGA 55, TA Instruments, DE, USA). The sample underwent heating from room temperature to 700°C under N<sub>2</sub> gas, at a rate of 10°C/min, with N<sub>2</sub> injected at a rate of 50 cm<sup>3</sup>/min. Approximately 5 mg of the sample was utilized for the analysis. The heating process involved ramping from room temperature to 700°C under N<sub>2</sub> gas, maintaining a rate of 10°C/min, and concurrent injection of N<sub>2</sub> at a rate of 50 cm<sup>3</sup>/min.

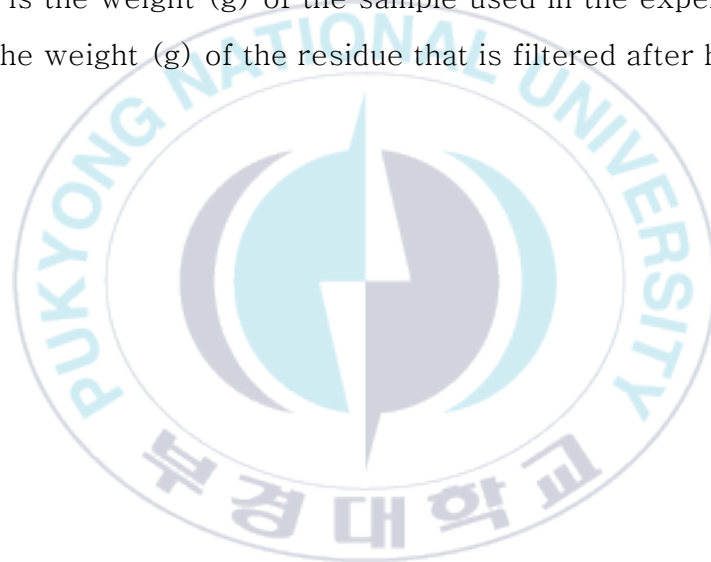
## 6. Subcritical water hydrolysis (SWH)

The sample utilized was skipjack tuna powder from which lipids were removed after SC-CO<sub>2</sub> extraction. Skipjack tuna hydrolysate (STH) was obtained using subcritical water extraction equipment made of Hastelloy 276 (Phosentech, Korea). The equipment, as illustrated in Figure 4, comprised a 500 cm<sup>3</sup> batch-type reactor, a thermometer, pressure gauge, heating and cooling system, and stirrer. The extraction was conducted using 6 g of sample and 300 mL (1:50, w/v) of distilled water. The mixture was sealed in a reactor and maintained at an initial pressure of 4 MPa with nitrogen gas. The stirring speed was held at 150 rpm. Once the temperature of the extraction zone reached 160°C to 230°C, the reaction ran for 15 min. The STH extracted was filtered through filter paper using a Vacuum Pump V-100 (manufactured by BUCHI, Switzerland), and subsequently stored in a dark place at a

temperature of  $-4^{\circ}\text{C}$ . For further analysis, the STH underwent freeze-drying and was stored in a dark location at  $-70^{\circ}\text{C}$ . After filtering, the residue was thoroughly dried at  $50^{\circ}\text{C}$ , and the hydrolysis efficiency (%) was calculated using the formula below.

$$\text{Hydrolysis efficiency (\%)} = \frac{S - S_1}{S} \times 100$$

Where  $S$  is the weight (g) of the sample used in the experiment, and the  $S_1$  is the weight (g) of the residue that is filtered after hydrolysis.



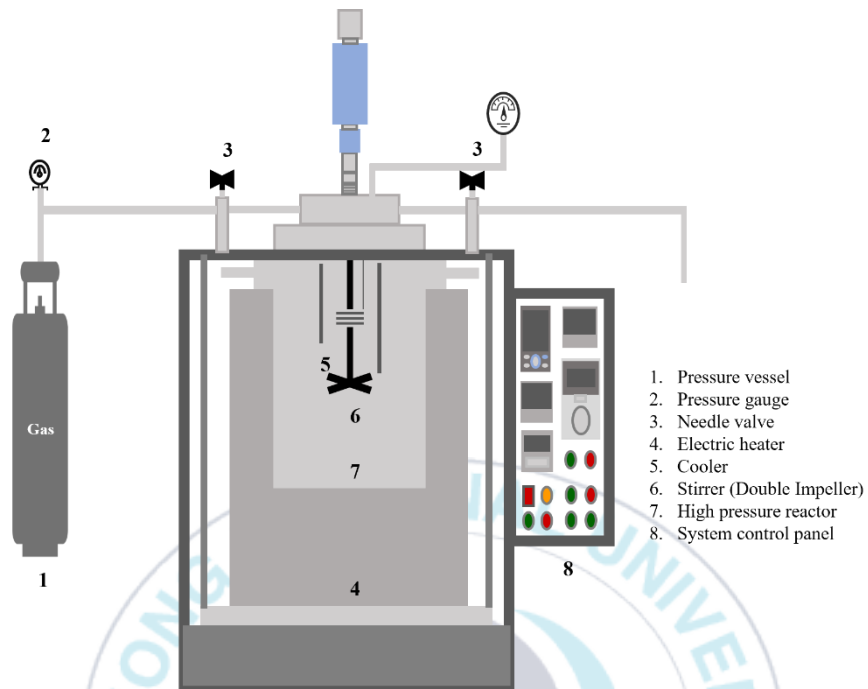


Figure 4. Schematic diagram of the subcritical water hydrolysis apparatus.

## 7. Analysis of physicochemical properties of hydrolysate

### 7.1. Color analysis

The colorimetric measurement of STH was performed using the same method as presented in Section 2.6.1.

### 7.2. pH analysis

The pH of the STH was measured using a pH meter (Orion Star A211, Thermo Scientific, USA). Before measurement, the pH buffer solutions (pH 4, pH 7, and pH 10) were calibrated to establish the standard values, and then the actual measurement of the samples was conducted. All samples were repeated three times and the average value was calculated.

### 7.3. Maillard reaction products (MRPs) measurements

The Maillard reaction products of STH were analyzed following the method outlined by Jeong Y. R. (2021) (Jeong et al., 2021). The sample comprised STH diluted five times with distilled water, and the absorbance was promptly measured at 420 nm using a spectrophotometer (Synergy HT, BioTek Instruments, Winousski, VT, USA). All samples

were repeated three times and the average value was calculated.

#### **7.4. Total sugar content measurements**

The total sugar content of STH was analyzed according to the method of Cho Y. J. (2019) (Cho et al., 2019). Add 2.25 mL of sulfuric acid and 0.45 mL of 40% phenol to a 15 mL tube containing 0.75 mL of STH and react at 95°C for 5 min. The absorbance was measured at 490 nm using a spectrophotometer, and the spectroscopy was conducted at room temperature. All samples were repeated three times and the average value was calculated. Glucose (GE) (Sigma–Aldrich Co., Ltd.) was used to create a standard curve.

#### **7.5. Reducing sugar content measurements**

The reducing sugar content of STH was determined using the 3,5–dinitrosalicylic acid (DNS) colorimetric method, following the procedure outlined by Cho Y. J. (2019) (Cho et al., 2019). For the preparation of the DNS solution, 5 g of DNS and 150 g of sodium potassium tartrate (Rochelle salt) were dissolved in 400 mL of 0.5 N NaOH, and distilled water was added to achieve a final volume of 500 mL. 4 mL of DNS solution were mixed with 1 mL of STH and reaction was reacted at 95°C for 5 min. Absorbance was measured at 540 nm using a spectrophotometer, and all samples were analyzed in triplicate. Glucose

(Sigma–Aldrich Co., USA) was used as the standard substance to establish a calibration curve for quantification.

#### **7.6. Total protein content measurements**

The water–soluble protein content of STH was determined following the method described by Park J. S. (2019) (Park et al., 2019). For the preparation of solution A of Lowry's reagent, 0.4 g of NaOH and 2 g of Na<sub>2</sub>CO<sub>3</sub> were dissolved in 80 mL of distilled water and diluted to a final volume of 100 mL. Solution B was prepared by dissolving 50 mg of cupric sulfate and 0.1 g of potassium sodium tartrate in 8 mL of distilled water. The final Lowry solution was obtained by combining solutions A and B in a 50:1 ratio. The FC reagent was prepared by mixing 2 N FC reagent and water in equal parts. Subsequently, 0.6 mL of STH was mixed with 3 mL of Lowry solution, stirred, and allowed to react in the dark for 20 min. Following the completion of the reaction, 300  $\mu$ L of FC reagent was added, stirred, and allowed to react in the dark for an additional 35 min. The absorbance was then measured at 750 nm using a spectrophotometer, and the entire procedure was repeated three times. A calibration curve was generated using Bovine serum albumin (BSA) from Sigma–Aldrich Co. as the reference material.

#### **7.7. Sodium dodecyl sulfate–polyacrylamide gel electrophoresis (SDS–PAGE) analysis**

To determine the molecular weight of proteins in STH, SDS-PAGE was performed using an electrophoresis device (PowerPac Basic Power Supply, BioRad, USA). The procedure was adapted from Jeong Y. R. (2021), with modifications (Jeong et al., 2021). The gel consisted of a 12% resolving gel and a 5% stacking gel. The running buffer was prepared by mixing 70 mL of Tris-Glycine SDS buffer (10X) with 700 mL of distilled water. The sample was prepared by adding 0.5 mL of HPLC water and 0.5 mL of loading buffer to 50 mg of the test material. The mixture was then heated to 95°C for 5 min and subsequently cooled in an ice bath. A 5  $\mu$ L volume of the sample was loaded into the Mini-PROTEIN Tetra cell, and electrophoresis was conducted at 120 V for 1 h 30 min. The resulting gel was separated, stained in a staining buffer for 1 h, and then destained in a destaining buffer. The Protein Ladder (ab116028, Abcam) was used as the standard material.

#### **7.8. Fourier transform infrared (FT-IR) spectrum analysis of hydrolysate**

FT-IR spectra were obtained using an FT-IR spectrometer (Jasco-4100, Jasco Corporation, Tokyo, Japan) with a resolution of better than 0.15  $\text{cm}^{-1}$  in the range of 500–4000  $\text{cm}^{-1}$ .

#### **7.9. Amino acid analysis**

### 7.9.1. Constituent amino acids analysis

To analyze the amino acids in DST powder and STH, we followed the method outlined by Henderson J. W. (2000) (Henderson et al., 2000). Sample preparation involved mixing 0.1 g of the sample with 10 mL of 6 N HCl and digesting it at 110°C for 24 h. Afterward, it was neutralized with sodium hydroxide to adjust the pH to approximately 7.0. Subsequently, the sample was diluted with 50 ml of tertiary distilled water, filtered through a 0.45  $\mu$ m hydrophilic syringe filter, and subjected to analysis using HPLC. The HPLC system comprised a Dionex Ultimate 3000 (pump, autosampler, oven, and ultraviolet [UV]; Thermo Fisher Scientific, Waltham, MA, USA) system equipped with a 1260FL fluorescence detector (Agilent, Santa Clara, CA, USA). Samples were separated using VDSpher 100 C<sub>18</sub>-E (46.6 mm  $\times$  150 mm, 3.5  $\mu$ m; Opti-Lab, Munich, Germany) as the column. The mobile phase solvent A was 40 mM sodium phosphate (pH 7), and solvent B was tertiary distilled water:acetonitrile:methanol (10:45:45, v/v%). The analysis time was 35 min, the column temperature was maintained at 40°C, the sample temperature was maintained at 20°C, and 0.5  $\mu$ L was injected. The fluorescence detector detected OPA (o-phthalaldehyde) at Emission 450 nm and Excitation 340 nm, and FMOC (fluorenylmethyloxycarbonyl chloride) at Emission 305 nm and Excitation 266 nm.

### 7.9.2. Free amino acids analysis

To analyze the amino acids in DST powder and STH, we followed the method outlined by Henderson J. W. (2000) (Henderson et al., 2000). To quantify the concentration of free amino acids, 0.5 g of the sample were combined with 7.5 mL of a 70% ethanol solution. The mixture was sonicated for an 1 h and left at room temperature for 24 h. The resulting solution was then filtered through a 0.20  $\mu$ m hydrophilic syringe filter and subsequently analyzed using HPLC. The HPLC analysis was conducted under the same conditions as the constituent amino acids, and free amino acids were detected through UV detection at 338 nm.

## **8. Physiological activity of hydrolysate**

### **8.1. Antioxidant activities of hydrolysate**

#### **8.1.1. DPPH radical scavenging activity**

The DPPH assay was conducted with slight modifications following the procedure outlined by Cho Y. J. (2019) (Cho et al., 2019). For the assay, a 0.1 mM DPPH solution was prepared, and 100  $\mu$ L of STH was added to 3.9 mL of the solution. The mixture was stirred for 30 s and left to react in the dark for 30 min. Measurements were taken three times at a wavelength of 517 nm using a spectrophotometer. The DPPH radical scavenging activity was expressed as mg Trolox equivalent (TE)/g of dried sample, with the Trolox standard curve utilized

(Sigma–Aldrich Co., USA).

### 8.1.2. ABTS<sup>+</sup> radical scavenging activity

The ABTS<sup>+</sup> radical scavenging activity of STH was determined using Jeong Y. R.'s (2021) method with some modifications (Jeong et al., 2021). To prepare the ABTS<sup>+</sup> stock solution, equal volumes of 7 mM ABTS solution and 2.45 mM potassium persulfate were mixed and kept in the dark for 16 h. The resulting solution was then diluted with methanol until an absorbance of  $0.74 \pm 0.02$  was obtained at 734 nm. For analysis, 3.9 mL of ABTS<sup>+</sup> solution and 100  $\mu$ L of the STH were mixed. After stirring for 30 s, the solution was allowed to react in darkness for 6 min. The standard curve was constructed using Trolox (Sigma–Aldrich Co., USA). The ABTS<sup>+</sup> radical scavenging activity is expressed as mg Trolox equivalent (TE)/g dried sample.

### 8.1.3. Ferric reducing antioxidant power (FRAP)

The ferric ion reducing power of STH was tested using the method of Belwal T. (2016) (Belwal et al., 2016). The preparation of the FRAP solution involved combining acetate buffer (pH 3.6) at a concentration of 300 mM, a 10 mM TPTZ solution, and 20 mM FeCl<sub>3</sub> · 6H<sub>2</sub>O in a ratio of 10:1:1. On the day of testing, 2.85 mL of the freshly prepared FRAP solution was mixed with 0.15 mL of the STH and incubated at 37 °C for

10 min. Absorbance was measured at a wavelength of 593 nm with a spectrophotometer, followed by the plotting of a standard curve using Trolox (Sigma–Aldrich Co., USA). The FRAP activity was then reported as mg Trolox equivalent (TE)/g of dried sample.

## 8.2. Antidiabetic activity

The antidiabetic activity of STH was evaluated through an in vitro analysis of  $\alpha$ –glucosidase inhibitory activity. Initially, lyophilized STH was diluted with potassium phosphate buffer (pH 6.8). Subsequently, 50  $\mu$ L of the sample was mixed with 50  $\mu$ L of 200 mM potassium phosphate buffer and 0.2 U/mL  $\alpha$ –glucosidase (dissolved in 200 mM potassium phosphate buffer) and then incubated at 37°C for 10 min. Following the incubation period, 100  $\mu$ L of 3 mM  $\rho$ –NPG was added, and the mixture was further incubated at 37°C for an additional 10 min. Absorbance was measured at 405 nm, and the inhibition rate was calculated using the provided formula. To account for any potential impact on the color of the sample solution, 50  $\mu$ L of the sample was combined with 200 mM potassium phosphate buffer and measured concurrently. Acarbose was used as the standard substance, and the IC<sub>50</sub> value, representing the sample solution's concentration required to achieve 50% inhibition of enzyme activity, was calculated by diluting the sample solution within the range of 0.1–20 mg/mL, following the same procedure as described above.

$$\text{Inhibition (\%)} = \left(1 - \frac{A_s - A_b}{A_c}\right) \times 100$$

where  $A_b$  is the color absorbance of the sample,  $A_c$  is the control absorbance, and  $A_s$  is the absorbance of the sample solution.

### 8.3. Anti-inflammatory activity

The STH in vitro anti-inflammatory activity was determined, following Chamika, W. A. S. (2021) (Chamika et al., 2021). The sample underwent preparation as a 1% freeze-dried powder through SWE. Fresh egg yolk albumin solution was created with 6.6% v/v (pH 6.4) of egg yolk in PBS. 500  $\mu$ L of sample had 2.5 mL of fresh egg yolk albumin solution added. The mixture was incubated at 37°C for 15 min, heated at 70°C for 5 min, and then cooled to room temperature. The absorbance was then measured at 660 nm utilizing a spectrophotometer. Distilled water served as the control group, while aspirin (500  $\mu$ g/mL) was employed as the standard substance. The protein denaturation inhibition rate was calculated applying the subsequent formula.

$$\text{Inhibition (\%)} = \left(\frac{A_c - A_s}{A_c}\right) \times 100$$

Where,  $A_c$  is the absorbance of the control solution, and  $A_s$  is the absorbance of the sample solution.

## 9. Statistical analysis

The data presented in this study were expressed as the mean  $\pm$  standard deviation of three measurements. All statistical treatments were statistically analyzed by SPSS (version 27.0, SPSS Inc., Chicago, IL, USA) using Duncan's multiple comparison analysis, where  $p < 0.05$  was considered significant.



### III. Result and Discussion

#### 1. Proximate compositions of *K. pelamis*

The proximate compositions of freeze-dried raw sample and DST by SC-CO<sub>2</sub> are shown in Table 5. The proximate compositions of raw sample, including its head, viscera, and skin, exhibited varying percentages of moisture (4.35% ± 0.26%, 8.61% ± 0.71%, 4.68% ± 0.85%), ash (21.15% ± 2.18%, 14.81% ± 0.15%, 17.01% ± 1.55%), crude protein (44.94% ± 0.90%, 57.73% ± 0.96%, 43.75% ± 0.41%), crude fat (16.07% ± 0.74%, 19.00% ± 0.46%, 34.78% ± 0.73%), and carbohydrate (11.39% ± 0.72%, 0.89% ± 0.05%, 0.87% ± 0.04%), indicating a high protein content. The protein content was highest in the viscera, while crude fat content was highest in the skin. The DST components, from which oil was removed using SC-CO<sub>2</sub>, contained moisture (1.99% ± 0.24%, 1.89% ± 0.19%, 1.51% ± 0.12%) and ash (20.93% ± 0.96%, 10.23% ± 1.98%, 9.91% ± 2.10%), crude protein (54.26% ± 0.88%, 75.30% ± 0.38%, 85.09% ± 0.50%), crude fat (4.59% ± 0.54%, 2.93% ± 0.99%, 1.10% ± 0.26%), and carbohydrates (18.23% ± 0.21%, 9.65% ± 0.14%, 2.39% ± 0.25%). After removing the oil, the crude protein content of the material relatively increased in this study, making it a suitable substance for lipid extraction and protein recovery.

Table 5. Proximate compositions of *K. pelamis* by-products

Composition	Raw material (%)			After SC-CO <sub>2</sub> extraction (%)		
	Head	Viscera	Skin	Head	Viscera	Skin
Moisture	4.35±0.26 <sup>e</sup>	8.61±0.71 <sup>d</sup>	4.68±0.85 <sup>d</sup>	1.99±0.24 <sup>e</sup>	1.89±0.19 <sup>c</sup>	1.51±0.12 <sup>c</sup>
Ash	21.15±2.18 <sup>b</sup>	14.81±0.15 <sup>c</sup>	17.01±1.55 <sup>c</sup>	20.93±0.96 <sup>b</sup>	10.23±1.98 <sup>b</sup>	9.91±2.10 <sup>b</sup>
Crude Protein	44.94±0.90 <sup>a</sup>	57.73±0.96 <sup>a</sup>	43.75±0.41 <sup>a</sup>	54.26±0.88 <sup>a</sup>	75.30±0.38 <sup>a</sup>	85.09±0.50 <sup>a</sup>
Crude Lipid	16.07±0.74 <sup>c</sup>	19.00±0.46 <sup>b</sup>	34.78±0.73 <sup>b</sup>	4.59±0.54 <sup>d</sup>	2.93±0.99 <sup>c</sup>	1.10±0.26 <sup>c</sup>
Carbohydrate	11.39±0.72 <sup>d</sup>	0.89±0.05 <sup>e</sup>	0.87±0.04 <sup>e</sup>	18.23±0.21 <sup>c</sup>	9.65±0.14 <sup>b</sup>	2.39±0.25 <sup>c</sup>

- Values are expressed as Mean ± SD (n=3).

- Different letters indicate significant differences (p<0.05).

## 2. Yield and purity of *K. pelamis* lipids

The lipid extraction yield from different parts using SC-CO<sub>2</sub> is displayed in Table 6. The raw sample oil yield was 14.20% ± 0.67% (Head oil, HO), 13.79% ± 1.05% (Viscera oil, VO), and 31.18% ± 0.59% (Skin oil, SO), with SO exhibiting twice the yield. Variations in extraction conditions were observed to affect oil extraction yield during SC-CO<sub>2</sub> extraction. The density of SC-CO<sub>2</sub>, which depends on the solubility of the solute in the solvent (Sarker et al., 2012), causes a complex impact on temperature, pressure, and flow rate. Consequently, differences in yield will occur depending on the extraction conditions. Further research is required to analyze the yield differences by condition. SC-CO<sub>2</sub> is efficient in the post-treatment process and time efficiency compared to organic solvents. Its low critical temperature makes it oxidation stable during the extraction of heat-sensitive compounds. Therefore, it is considered a suitable method for extracting oil from skipjack tuna (Ishak et al., 2021). The extraction yields of PLs using SC-CO<sub>2</sub> and co-solvent ethanol were 5.87% ± 0.47% (Head PLs, HP), 4.15% ± 0.04% (Viscera PLs, VP), and 2.80% ± 0.44% (Skin PLs, SP), respectively. PLs were not detected in the purity analysis of the extracted oil. However, the extracted PLs yielded at 58.53% ± 0.04%, 59.00% ± 0.06%, and 54.09% ± 0.05%. Additionally, pure PLs obtained by applying purity were 3.24%, 2.47%, and 1.68%, with the highest yield obtained from the head. Fish brain is known to be rich in PLs, consistent with Ahmmed M. K.'s (2021) research (Kreps et al., 1975; Ahmmed et al., 2021). Haq and Chun (2018) found that SC-CO<sub>2</sub> extraction of PLs has high selectivity compared to conventional organic

solvent extraction, which has lower purity. The use of SC-CO<sub>2</sub> extraction can produce high-quality PLs suitable for use in food. Therefore, this extraction method is a suitable option.

The color of oil is a significant factor in food quality. It serves as a crucial quality indicator for oil. The color measurement results for the oil extracted using SC-CO<sub>2</sub> for each part are shown in the table (Table 7). Notably, the VO yielded a high a\* value of  $15.59 \pm 0.33$ , displaying a distinct red color. The L\* values indicate that the oil is generally brightly yellow with the highest value observed in the HO ( $53.99 \pm 0.38$ ,  $42.99 \pm 1.17$ ,  $43.84 \pm 0.73$ ). Lee et al. (2022) reported that oil extracted through SC-CO<sub>2</sub>, a non-polar solvent that employs highly selective CO<sub>2</sub>, displays relatively yellow and bright characteristics.

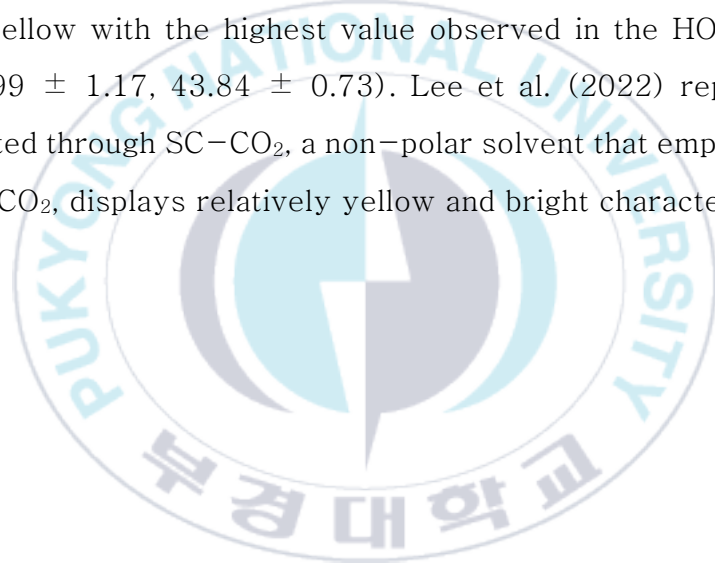


Table 6. Yield, purity content of lipid extracted from *K. pelamis*

Parameters	Head		Viscera		Skin	
	HO	HP	VO	VP	SO	SP
Yield (%)	14.20±0.67 <sup>b</sup>	5.87±0.47 <sup>a</sup>	13.79±1.05 <sup>b</sup>	4.15±0.04 <sup>b</sup>	31.18±0.59 <sup>a</sup>	2.80±0.44 <sup>c</sup>
Purity (%)	58.53±0.04 <sup>b</sup>	N.D	59.00±0.06 <sup>a</sup>	N.D	54.09±0.05 <sup>c</sup>	N.D
Net PL obtained (%)	3.24		2.47		1.68	

– N.D.: Not detected.

– Values are expressed as Mean ± SD (n=3).

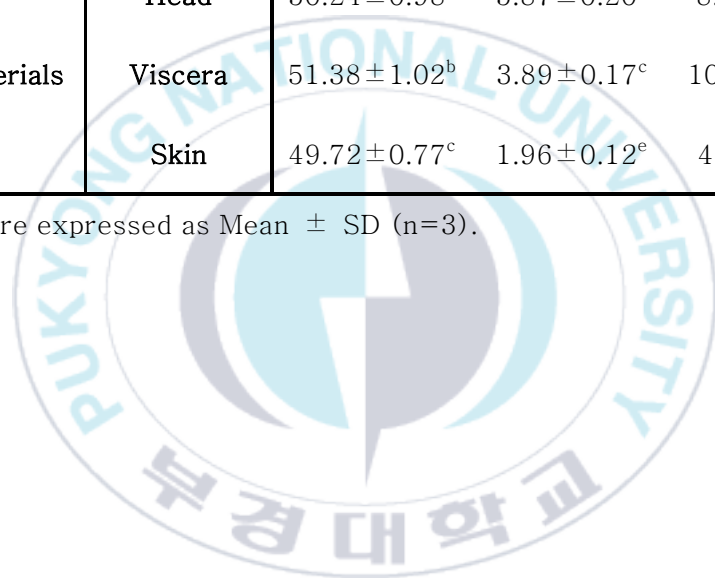
– Total PL yield=Lecithin yield (%) x PL (% of lecithin) / 100.

– HO, head oil of *K. pelamis*; VO, viscera oil of *K. pelamis*; SO, skin oil of *K. pelamis*; HP, head phospholipid of *K. pelamis*; VP, viscera phospholipid of *K. pelamis*; SP, skin phospholipid of *K. pelamis*.

Table 7. Color properties of oils extracted from *K. pelamis*

Conditions	Parts	L*	a*	b*
Oils	Head	53.99±0.38 <sup>a</sup>	3.43±0.04 <sup>d</sup>	35.44±0.28 <sup>a</sup>
	Viscera	42.99±1.17 <sup>d</sup>	15.59±0.33 <sup>a</sup>	21.8±0.49 <sup>b</sup>
	Skin	43.84±0.73 <sup>d</sup>	0.01±0.04 <sup>f</sup>	14.28±0.65 <sup>c</sup>
Raw materials	Head	50.24±0.98 <sup>c</sup>	5.87±0.20 <sup>b</sup>	8.60±0.62 <sup>e</sup>
	Viscera	51.38±1.02 <sup>b</sup>	3.89±0.17 <sup>c</sup>	10.91±0.53 <sup>d</sup>
	Skin	49.72±0.77 <sup>c</sup>	1.96±0.12 <sup>e</sup>	4.48±0.29 <sup>f</sup>

– Values are expressed as Mean ± SD (n=3).



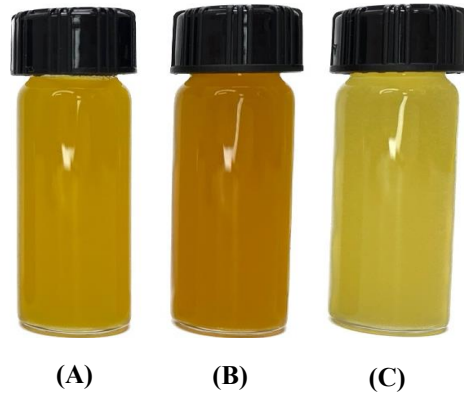
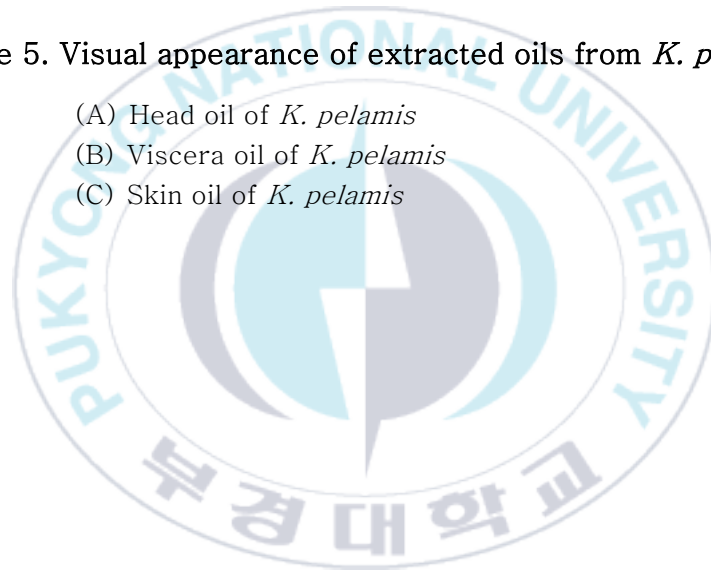


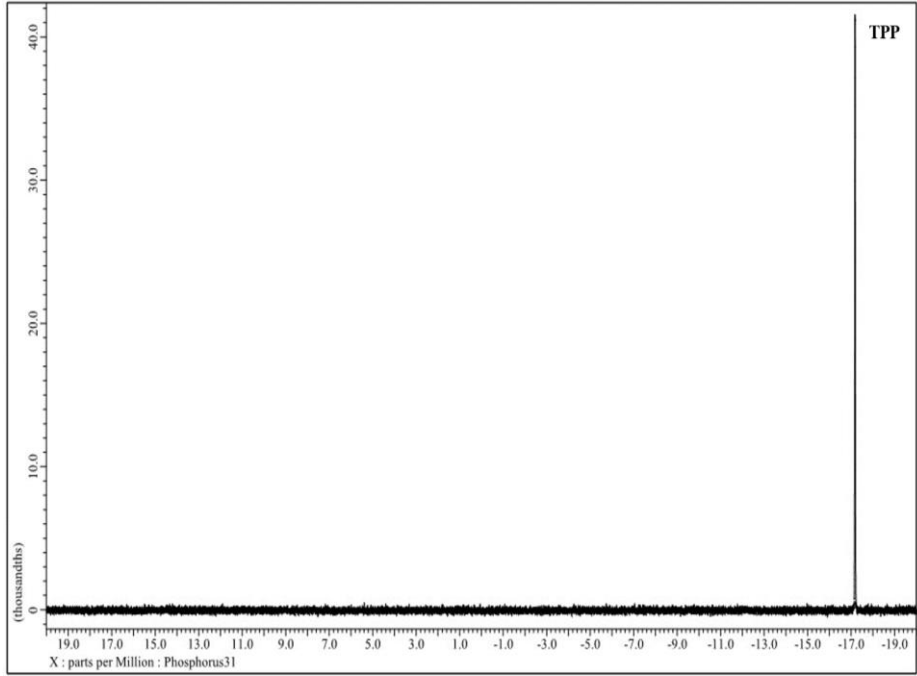
Figure 5. Visual appearance of extracted oils from *K. pelamis*.

- (A) Head oil of *K. pelamis*
- (B) Viscera oil of *K. pelamis*
- (C) Skin oil of *K. pelamis*

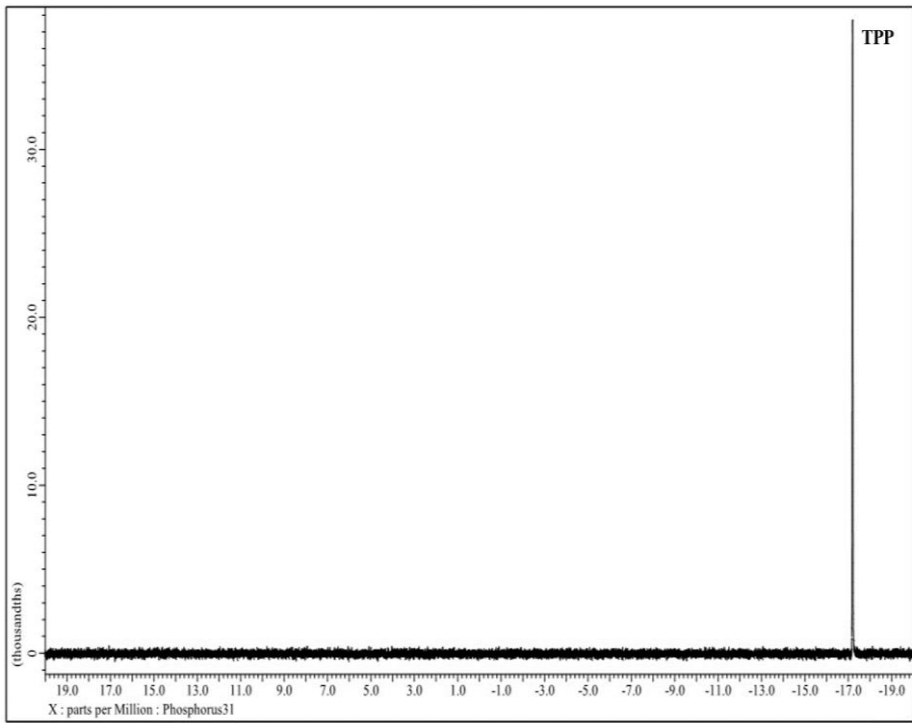


### 3. PLs composition of *K. pelamis* by $^{31}\text{P}$ NMR

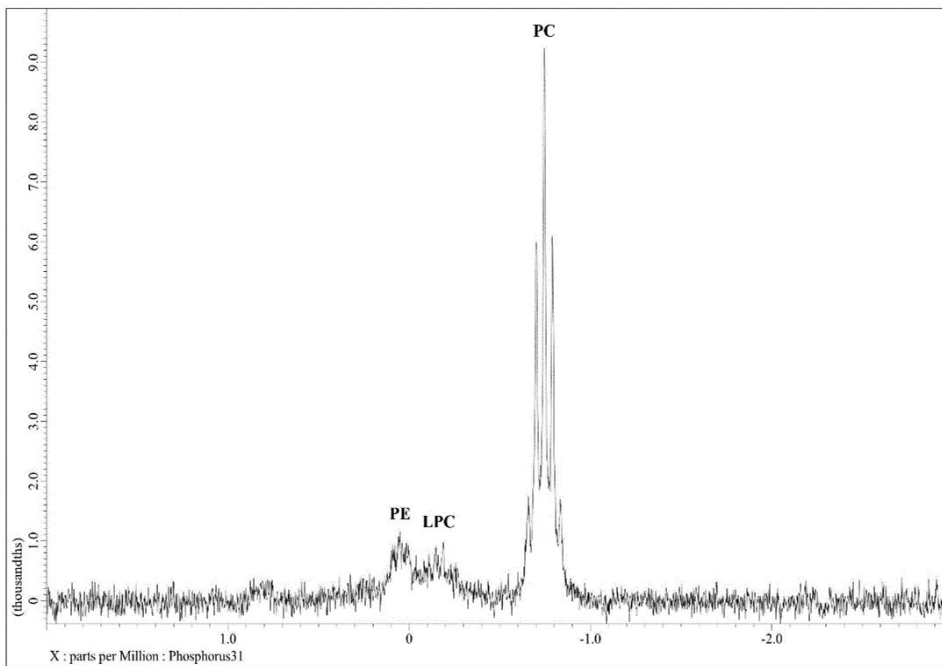
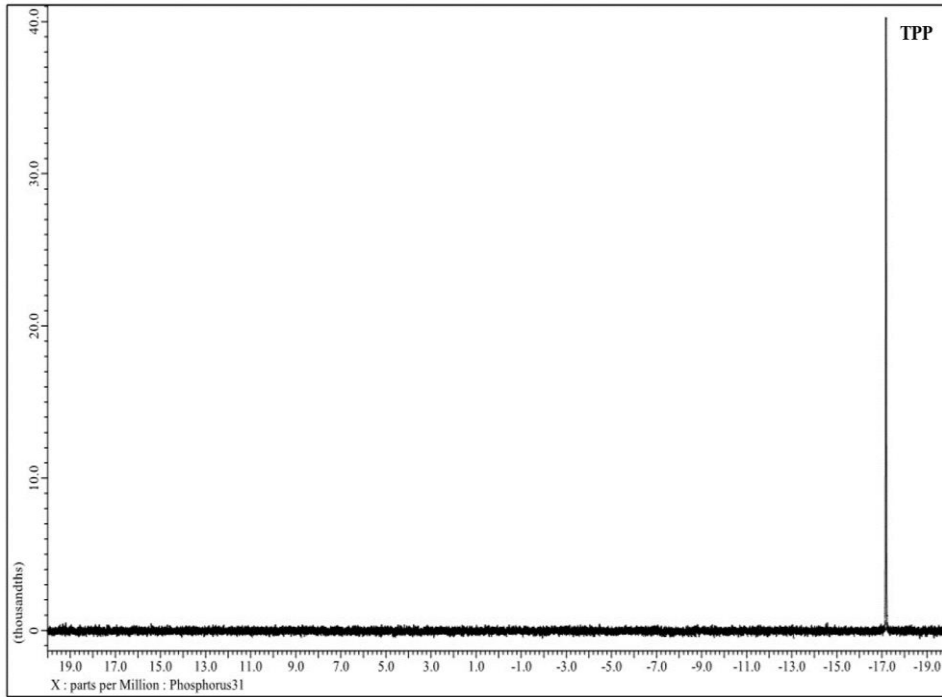
The  $^{31}\text{P}$  NMR serves for both qualitative and quantitative analyses of PLs. Figure 6 displays the NMR spectra, and Table 8 summarizes the PLs chemical shifts and content relative to the internal standard TPP ( $\delta -17.8$ ). The spectrum was identified by comparing it with the spectra of egg yolk and soy lecithin (Figure 6). The primary lipid classes identified based on parts were phosphatidylcholine (PC), phosphatidylethanolamine (PE), and lysophosphatidylcholine (LPC), with a small quantity of cardiolipin (CD) observed in the SP. The HP samples showed measurements of  $490.38 \mu\text{mol/g}$  (PC),  $104.17 \mu\text{mol/g}$  (LPC), and  $82.26 \mu\text{mol/g}$  (PE). The VP yielded results of  $1875.69 \mu\text{mol/g}$  (PC),  $257.45 \mu\text{mol/g}$  (LPC), and  $159.37 \mu\text{mol/g}$  (PE). The SP contained  $637.49 \mu\text{mol/g}$  (PC),  $43.25 \mu\text{mol/g}$  (LPC), and  $122.59 \mu\text{mol/g}$  (PE), with  $25.57 \mu\text{mol/g}$  (CD) being detected as well. PC was identified as the most prevalent class, constituting over 70% (72.15%, 81.82%, and 79.36%) in all parts. Furthermore, the total PLs content was significantly higher in the VP, measuring  $2292.51 \mu\text{mol/g}$ , consistent with the findings of Shoeb Z. E.'s study (Shoeb et al., 1973). Moreover, after comparing with egg yolk and soy lecithin, it was confirmed that the PLs obtained through SC-CO<sub>2</sub> had a simple composition. This is thought to be due to the selective extraction of PLs depending on the temperature, pressure, and cosolvent properties during extraction with SC-CO<sub>2</sub> (Teberikler et al., 2001).

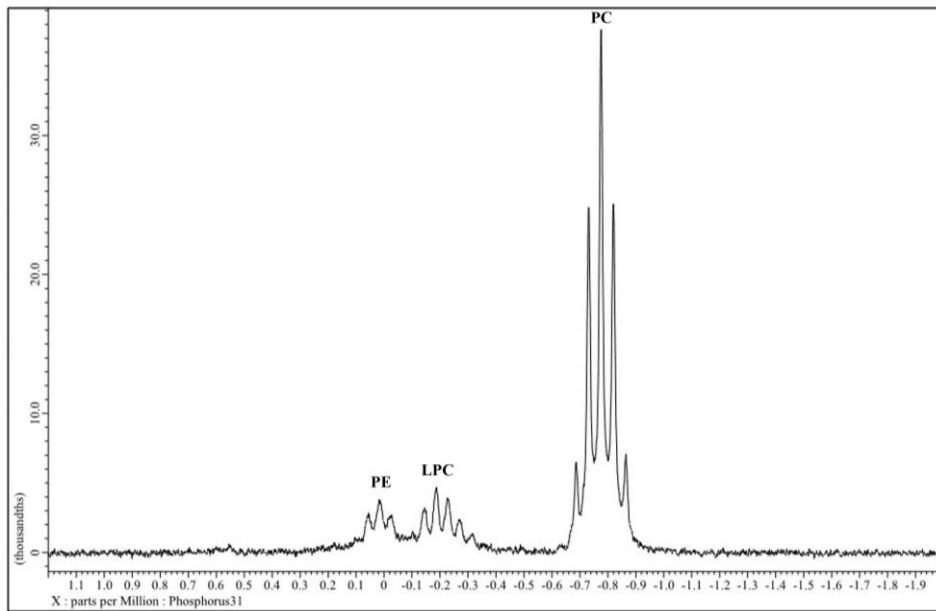


(A)

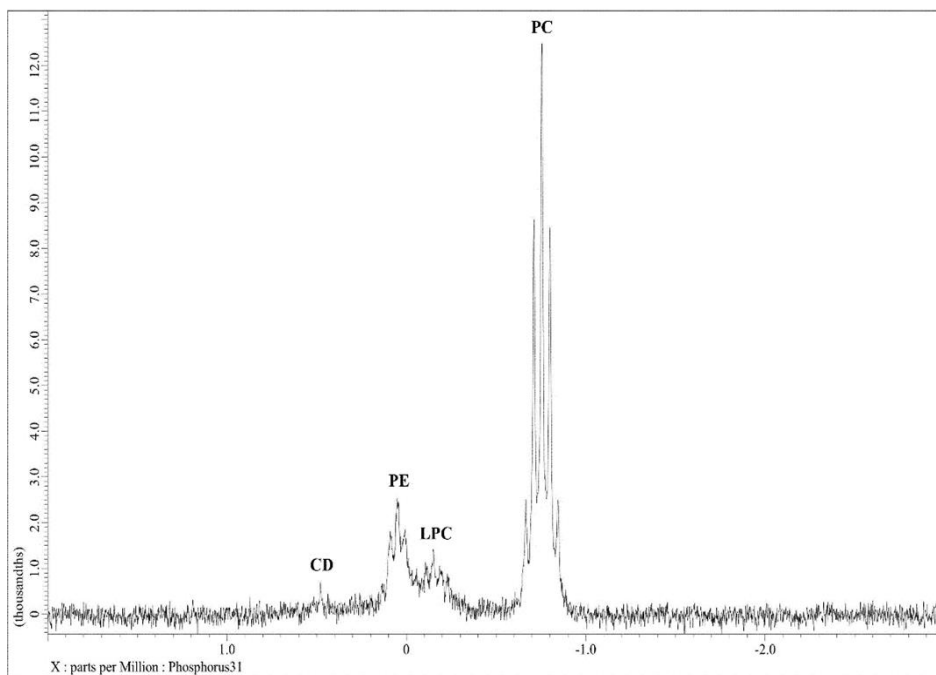


(B)

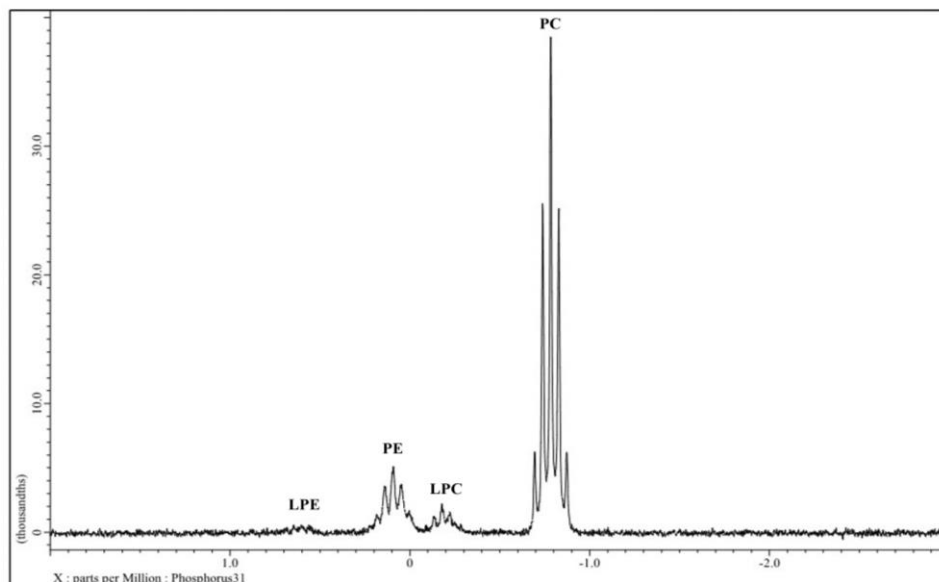




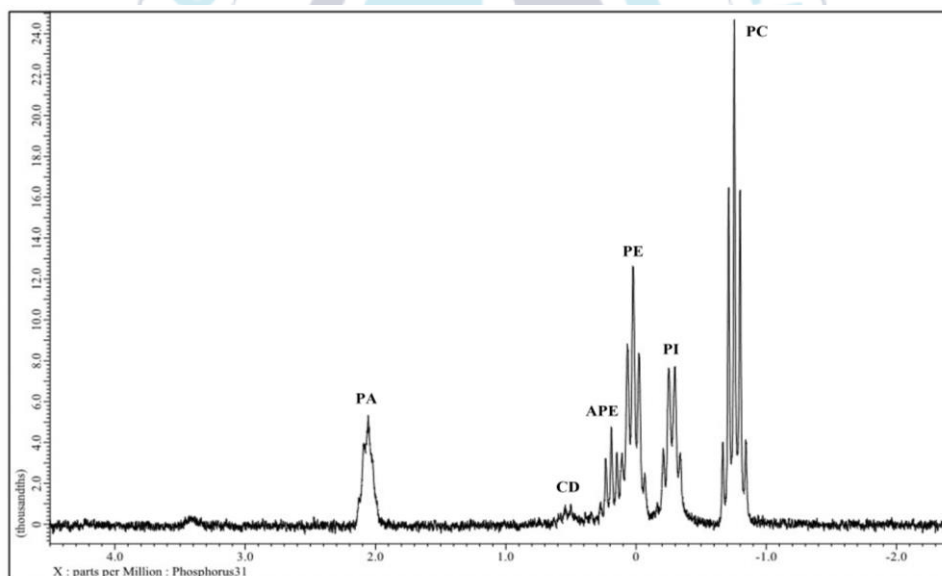
(E)



(F)



(G)



(H)

Figure 6.  $^{31}\text{P}$  NMR spectra of phospholipid extracted from different parts of *K. pelamis*.

(A) Head oil of *K. pelamis*; (B) Viscera oil of *K. pelamis*; (C) Skin oil of *K. pelamis*; (D) Head phospholipid of *K. pelamis*; (E) Viscera phospholipid of *K. pelamis*; (F) Skin phospholipid of *K. pelamis*; (G) Commercial egg yolk lecithin; (H) Commercial soy lecithin.

Table 8. Phospholipid composition ( $\mu\text{mol/g}$  oil, %) of *K. pelamis* determined by  $^{31}\text{P}$  NMR

Phospholipid composition	Phospholipids			Commercial phospholipids	
	HP	VP	SP	EL	SL
PA	N.D.	N.D.	N.D.	N.D.	2991.30 (12.66)
LPE	N.D.	N.D.	N.D.	30.81 (1.46)	N.D.
CD	N.D.	N.D.	25.57 (2.78)	N.D.	588.45 (2.49)
APE	N.D.	N.D.	N.D.	N.D.	2317.03 (9.8)
PE	82.26 (12.15)	159.37 (6.95)	122.59 (15.26)	416.82 (19.71)	5173.47 (21.89)
PI	N.D.	N.D.	N.D.	N.D.	4952.80 (20.095)
LPC	104.17 (15.39)	257.45 (11.23)	43.25 (5.38)	109.97 (5.20)	N.D.
PC	490.38 (72.15)	1875.69 (81.82)	637.49 (79.36)	1556.94 (73.63)	7613.09 (32.21)
<b>Total</b>	676.81	2292.51	993.0121	2114.54	23636.14

- N.D.: Not detected.
- EL, egg lecithin; SL, soybean lecithin.
- HP, head phospholipid of *K. pelamis*; VP, viscera phospholipid of *K. pelamis*; SP, skin phospholipid of *K. pelamis*.
- PA, phosphatidic acid; LPE, lysophosphatidylethanolamine; CD, cardiolipin; APE, N-acyl phosphatidylethanolamine; PE, phosphatidylethanolamine; PI, phosphatidylinositol; LPC, lysophosphatidylcholine; PC, phosphatidylcholine.

#### 4. Fatty acids composition of *K. pelamis* lipids

The fatty acid composition of the oil and PLs extracted using SC-CO<sub>2</sub> is detailed in Table 9 and Table 10. The predominant fatty acids in skipjack tuna were identified as palmitic acid, oleic acid, and docosahexaenoic acid (DHA), an  $\omega$ -3 fatty acid. Palmitic acid exhibited the highest content in the head, viscera, and skin, measuring 25.25%  $\pm$  0.61%, 31.70  $\pm$  0.71%, and 23.15%  $\pm$  0.42%, respectively. Following closely, DHA showed substantial presence at 23.08%  $\pm$  0.19%, 12.33%  $\pm$  1.87%, and 24.81%  $\pm$  1.04% in the same respective parts. Both oils and PLs demonstrated significant levels of polyunsaturated fatty acids (PUFA), particularly  $\omega$ -3 and  $\omega$ -6 fatty acids, primary components in marine lipids known for their diverse health benefits. The HO, VO, SO contained 28.26%, 15.74%, and 30.02% of  $\omega$ -3 PUFA, while PLs exhibited 7.89%, 15.82%, and 19.91% of  $\omega$ -3 fatty acids. Previous studies have underscored the efficacy of fish-derived  $\omega$ -3 fatty acids, especially EPA, in mitigating the risk of cardiovascular disease, promoting brain development, and offering various health advantages (Marik et al., 2009; Valentini et al., 2018). Additionally, PLs are known to possess diverse functional activities. The incorporation of  $\omega$ -3 and  $\omega$ -6 polyunsaturated fatty acids (PUFA) in MPLs sets them apart from plant PLs, enhancing their health benefits and underscoring their value as MPLs (Ahmmed et al., 2021a; Ahmmed et al., 2021b; Zhang et al., 2019).

Table 9. Fatty acid composition *K. pelamis* oil

Fatty acids (%)	Oil		
	HO	VO	SO
Myristic acid (C14:0)	5.10±0.53	2.84±0.07	3.99±0.57
Palmitic acid (C16:0)	25.25±0.61	31.70±0.71	23.15±0.42
Heptadecanoic acid (C17:0)	7.44±0.52	7.09±0.24	6.86±0.57
Stearic acid (C18:0)	7.84±0.27	9.37±1.01	7.56±0.06
Arachidic acid (C20:0)	0.61±0.09	0.62±0.07	0.76±0.30
Behenic acid (C22:0)	0.14±0.52	0.16±0.01	0.26±0.06
Lignoceric acid (C24:0)	0.01±0.02	0.02±0.09	0.02±0.18
<b>Saturated fatty acids</b>	<b>46.39</b>	<b>51.80</b>	<b>42.60</b>
Myristoleic acid (C14:1n-5)	1.72±0.30	1.08±0.74	1.37±0.12
Palmitoleic acid (C16:1n-7)	5.04±0.06	4.13±0.20	4.27±0.01
cis-10-Heptadecanoic acid (C17:1)	0.78±0.02	0.79±0.03	0.72±0.02
Oleic acid (C18:1cis-9)	10.82±0.38	2.48±0.03	2.15±0.08
Elaidic acid (C18:1trans-9)	0.50±0.78	17.48±0.72	11.51±0.80
Eicosenoic acid (C20:1)	0.55±0.77	0.79±0.09	0.77±0.16
Nervonic acid (C24:1n-9)	0.53±0.11	0.57±0.47	0.61±0.78
Erucic acid (C22:1)	0.10±0.07	0.05±1.09	0.10±0.07
<b>Monounsaturated fatty acids</b>	<b>20.04</b>	<b>27.37</b>	<b>21.50</b>
Linoleic acid (C18:2cis-9,12)	1.64±0.18	1.43±1.07	1.85±0.25
Linoelaidic acid (C18:2trans-9,12)	0.07±0.18	0.69±0.09	0.08±0.18
$\gamma$ -Linolenic acid (C18:3cis-6,9,12)	0.19±0.58	0.31±0.99	0.4±0.04
Eicosadienoic acid (C20:2cis-11,14)	1.09±0.20	0.66±0.12	1.13±0.01
Dihomo- $\gamma$ -linolenic acid (C20:4cis-5,8,11,14)	0.05±0.60	0.14±0.08	0.10±0.01
Arachidonic Acid (C20:4cis-5,8,11,14)	1.83±0.06	1.47±0.76	1.84±0.10
Docosadienoic acid (C22:2cis-13,16)	0.44±0.18	0.39±0.08	0.49±0.39
<b><math>\omega</math>-6 Polyunsaturated fatty acids</b>	<b>5.31</b>	<b>5.09</b>	<b>5.89</b>
$\alpha$ -Linolenic acid (C18:3cis-9,12,15)	0.42±0.54	0.43±0.32	0.64±0.06
Eicosatrienoic acid (C20:3cis-11,14,17)	0.21±0.18	0.13±0.11	0.19±0.01
Eicosapentaenoic acid (C20:5cis-5,8,11,14,17)	4.55±0.24	2.85±1.31	4.38±0.01
Docosahexaenoic acid (C22:6cis-4,7,10,13,16,19)	23.08±0.19	12.33±1.87	24.81±1.04
<b><math>\omega</math>-3 Polyunsaturated fatty acids</b>	<b>28.26</b>	<b>15.74</b>	<b>30.02</b>

- Values are expressed as Mean  $\pm$  SD (n=3).

- HO, head oil of *K. pelamis*; VO, viscera oil of *K. pelamis*; SO, skin oil of *K. pelamis*.

Table 10. Fatty acid composition *K. pelamis* phospholipid

Fatty acids (%)	Phospholipid		
	HP	VP	SP
Myristic acid (C14:0)	3.95±0.02	1.55±0.71	1.98±0.11
Palmitic acid (C16:0)	30.54±0.02	33.19±0.02	19.46±1.07
Heptadecanoic acid (C17:0)	15.81±0.18	14.12±0.48	12.74±0.02
Stearic acid (C18:0)	9.95±0.96	7.00±0.55	8.68±0.06
Arachidic acid (C20:0)	1.31±0.01	0.54±0.88	0.67±0.34
Behenic acid (C22:0)	1.49±0.09	0.59±0.87	0.73±0.12
Lignoceric acid (C24:0)	1.75±0.72	0.71±1.08	0.88±0.11
<b>Saturated fatty acids</b>	<b>64.80</b>	<b>57.70</b>	<b>45.15</b>
Myristoleic acid (C14:1n-5)	0.93±0.51	0.25±0.44	0.35±0.08
Palmitoleic acid (C16:1n-7)	3.30±0.15	2.51±0.56	2.37±0.08
cis-10-Heptadecanoic acid (C17:1)	0.81±0.03	0.71±0.69	0.89±0.07
Oleic acid (C18:1cis-9)	8.39±0.04	12.13±0.69	3.49±0.10
Elaidic acid (C18:1trans-9)	0.55±0.02	0.34±0.04	15.04±0.01
Eicosenoic acid (C20:1)	0.89±0.21	0.64±0.18	0.79±0.58
Nervonic acid (C24:1n-9)	1.01±0.20	0.77±0.90	0.95±0.18
Erucic acid (C22:1)	0.77±0.12	0.40±0.01	0.50±0.01
<b>Monounsaturated fatty acids</b>	<b>16.66</b>	<b>17.75</b>	<b>24.38</b>
Linoleic acid (C18:2cis-9,12)	1.68±0.72	1.38±0.39	1.70±0.04
Linoelaidic acid (C18:2trans-9,12)	0.30±1.02	0.19±0.29	0.23±0.62
$\gamma$ -Linolenic acid (C18:3cis-6,9,12)	0.66±0.01	0.66±0.72	0.82±0.21
Eicosadienoic acid (C20:2cis-11,14)	1.57±0.06	0.62±0.09	0.74±0.21
Dihomo- $\gamma$ -linolenic acid (C20:4cis-5,8,11,14)	0.61±0.26	0.40±0.09	0.50±0.22
Arachidonic Acid (C20:4cis-5,8,11,14)	1.37±0.24	2.82±0.47	3.50±0.02
Docosadienoic acid (C22:2cis-13,16)	1.12±0.11	0.61±0.01	0.76±0.78
<b><math>\omega</math>-6 Polyunsaturated fatty acids</b>	<b>7.31</b>	<b>6.68</b>	<b>8.25</b>
$\alpha$ -Linolenic acid (C18:3cis-9,12,15)	0.99±1.01	0.12±0.77	0.43±0.51
Eicosatrienoic acid (C20:3cis-11,14,17)	0.76±0.89	0.32±0.15	0.40±0.14
Eicosapentaenoic acid (C20:5cis-5,8,11,14,17)	1.43±0.51	3.34±0.11	4.14±0.28
Docosahexaenoic acid (C22:6cis-4,7,10,13,16,19)	4.71±0.02	12.05±0.05	14.95±0.04
<b><math>\omega</math>-3 Polyunsaturated fatty acids</b>	<b>7.89</b>	<b>15.82</b>	<b>19.91</b>

- Values are expressed as Mean  $\pm$  SD (n=3).

- HP, head phospholipid of *K. pelamis*; VP, viscera phospholipid of *K. pelamis*; SP, skin phospholipid of *K. pelamis*.

## 5. Fat-soluble vitamins of *K. pelamis* lipids

The fat-soluble vitamin content of oil and PLs extracted via SC-CO<sub>2</sub> is displayed in Table 11. Retinol (vitamin A) and tocopherol (vitamin E) have distinct physiological activities within the human body. Retinol plays a definitive role in human growth and maintaining healthy vision but is unable to be synthesized within the human body (Underwood et al., 1996). A mere  $1.06 \pm 0.02$  mg/100g of retinol was detected solely in VO. Tocopherol, also known as vitamin E, acts as a potent antioxidant with anti-cancer and anti-inflammatory properties that aid in disease prevention in the human body (Colombo et al., 2010). Tocopherol plays a pivotal role in maintaining high lipid stability by thwarting radicals before they react with unsaturated fats. It is frequently added to marine products, particularly fish oil, and has been found to have a protective effect during food storage and processing (Afonso et al., 2016; Zuta et al., 2007). Tocopherol was present in high concentrations in both oil and PLs.  $\gamma$ -tocopherol displayed the highest concentration at  $29.73 \pm 0.13$  mg/100g,  $17.88 \pm 0.02$  mg/100g,  $76.57 \pm 0.84$  mg/100g in oil. In PLs, the concentrations were  $25.98 \pm 0.12$  mg/100g,  $18.90 \pm 0.11$  mg/100g,  $19.49 \pm 0.09$  mg/100g. Due to tocopherol's sensitivity to heat, the use of SC-CO<sub>2</sub> extraction for oil and PLs extraction can be an effective technique in extracting valuable lipids.

Table 11. Fat-soluble vitamin contents of lipids extracted from different parts of *K. pelamis*

Conditions		Retinol (mg/100g)	Tocopherol (mg/100g)			
			$\alpha$ -	$\beta$ -	$\gamma$ -	$\delta$ -
Oil	HO	N.D.	1.06±0.09	N.D.	29.73±0.13	0.16±0.01
	VO	1.06±0.02	0.68±0.03	N.D.	17.88±0.02	0.08±0.07
	SO	N.D.	3.86±0.20	N.D.	76.57±0.84	0.61±0.10
Phospholipid	HP	N.D.	1.23±0.06	N.D.	25.98±0.12	0.19±0.10
	VP	N.D.	0.96±0.03	N.D.	18.90±0.11	0.11±0.05
	SP	N.D.	1.64±0.05	N.D.	19.49±0.09	0.07±0.05

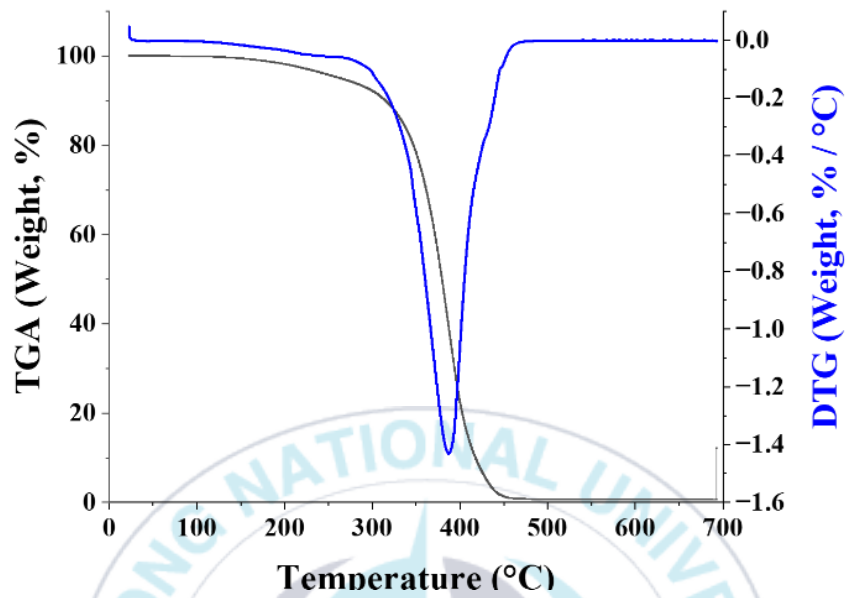
- N.D.: Not detected.

- Values are expressed as Mean  $\pm$  SD (n=3).

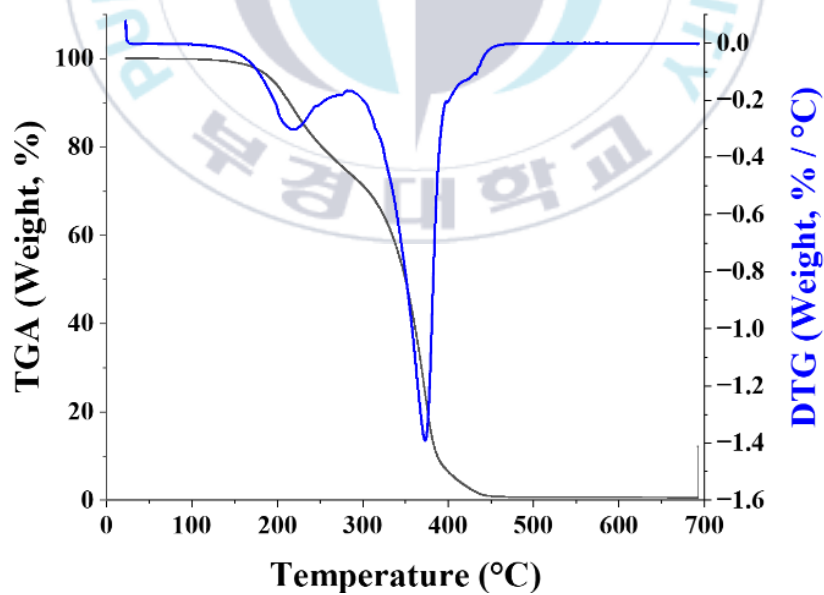
- HO, head oil of *K. pelamis*; VO, viscera oil of *K. pelamis*; SO, skin oil of *K. pelamis*; HP, head phospholipid of *K. pelamis*; VP, viscera phospholipid of *K. pelamis*; SP, skin phospholipid of *K. pelamis*.

## 6. Thermogravimetric analysis (TGA) of *K. pelamis* lipids

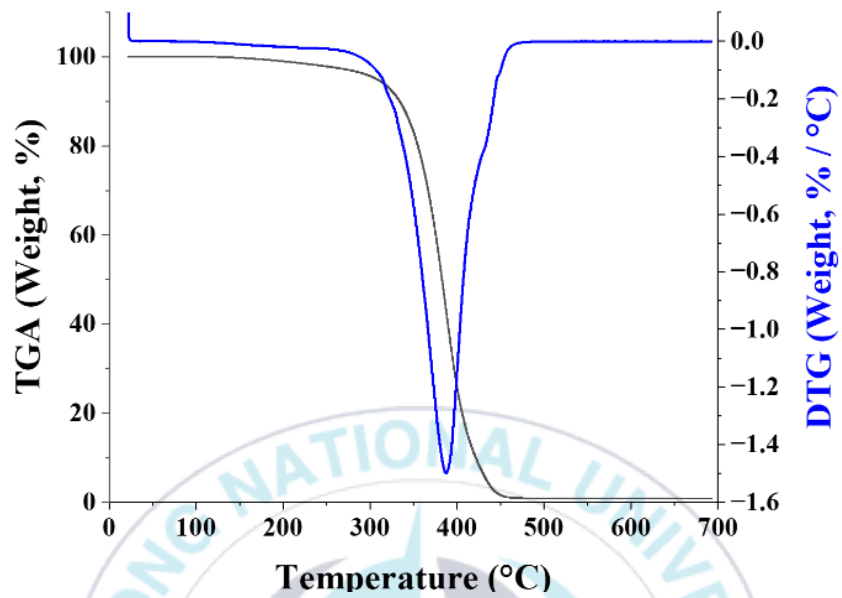
TGA was employed to assess the composition and thermal stability of the lipid samples. Figure 7 illustrates the TGA output graph of the extracted oil. TGA profiles may differ based on lipid composition, quality, and impurities present (Roy et al., 2022; Patil et al., 2018). The HO and SO displayed considerable weight loss at nearly 350°C, whereas VO exhibited a two-stage reduction at nearly 200°C and again at 350°C. The DTG curve for oil extracted from skipjack tuna reveals a decomposition curve at approximately 380–400°C, suggesting that the extracted oil can be utilized for various industrial purposes at room temperature (Roy et al., 2022). Moreover, the HO began to lose weight around 302.141°C and underwent significant weight loss, reaching a final weight of 0.631% at 600°C. The VO and SO also experienced a decrease in weight at 284.775°C and 314.923°C, showing a final weight of 0.609% and 0.765%, respectively. In the case of oil, it was confirmed that the majority of organic substances decomposed around 500°C. The TGA analysis results of the phospholipids revealed a weight loss that was more complex than the simple weight loss demonstrated in the oil. In HP, there were three stages of weight loss achieved at temperatures of 34.811°C, 55.766°C, and 301.615°C. VP and SP both exhibited four stages of weight loss at specific temperatures (VP: 32.238°C, 49.128°C, 288.802°C, 390.272°C; SP: 89.773°C, 209.124°C, 283.027°C, 397.329°C). This finding is consistent with previous research by Haq & Chun (2018), which also reported that the pyrolysis of phospholipids extracted from salmon bones shows rapid weight loss between 200°C and 450°C (Haq & Chun, 2018).



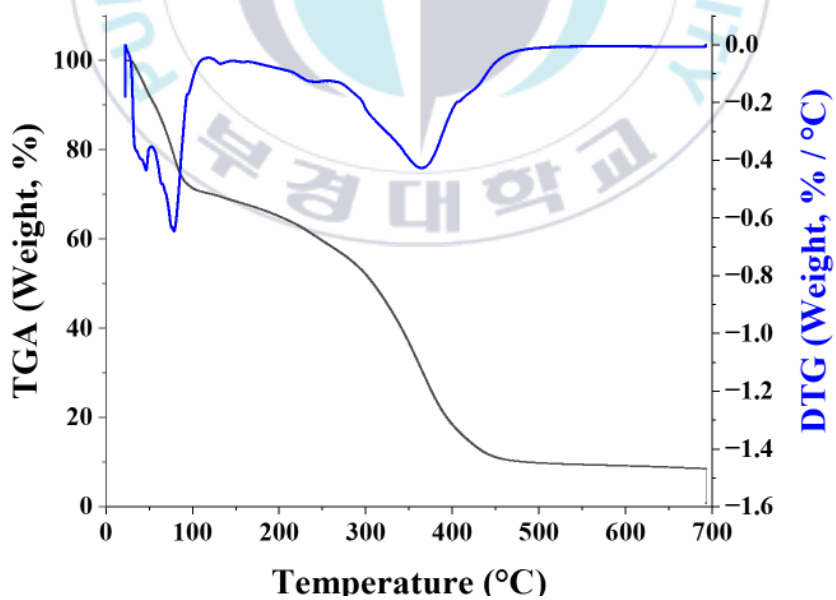
(A)



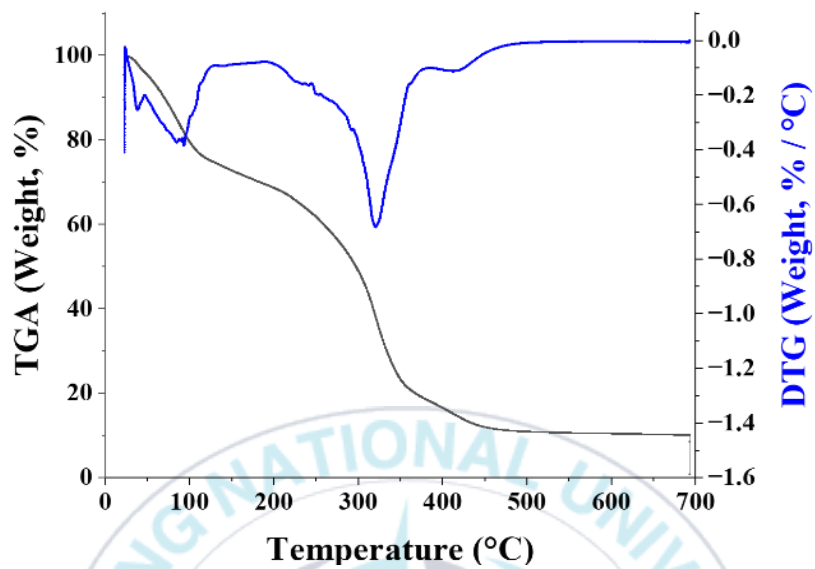
(B)



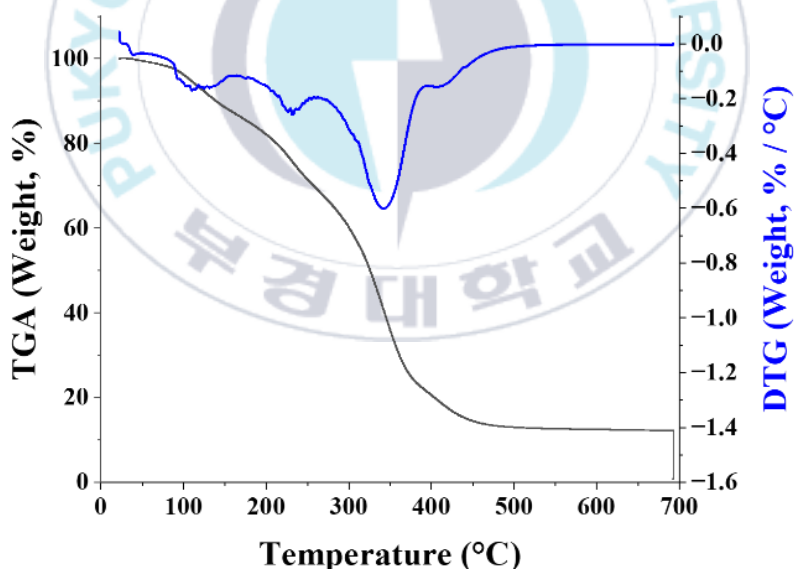
(C)



(D)



(E)



(F)

Figure 7. TGA (Thermogravimetric Analysis) of lipids extracted from different parts of *K. pelamis*.

(A) Head oil of *K. pelamis*; (B) Viscera oil of *K. pelamis*; (C) Skin oil of *K. pelamis*; (D) Head phospholipid of *K. pelamis*; (E) Viscera phospholipid of *K. pelamis*; (F) Skin phospholipid of *K. pelamis*.

## 7. Yield and MRPs of *K. pelamis* hydrolysate

Table 12 presents the yield of STH at varying temperatures. As the temperature increased, hydrolysis efficiency also tended to increase. At the highest temperature of 240°C, yield differences were 73.17%  $\pm$  0.39% (Head hydrolysate, HH), 90.17%  $\pm$  0.96% (Viscera hydrolysate, VH), and 79.50%  $\pm$  0.12% (Skin hydrolysate, SH), respectively. Notably, the VH produced the highest yield while the HH generated the lowest. The increase in yield is attributed to higher temperatures providing greater energy to break down peptide bonds, thereby facilitating the penetration of the solvent into the low molecular weight peptide sample (Ramachandraiah et al., 2017).

Maillard reaction products occur naturally during heat treatment via the interaction between reducing sugars and available amino acids. The process entails the creation of melanoidins, high molecular weight compounds that possess chromophores with an absorbance maximum at 420 nm. According to Table 13, MRPs tended to rise with temperature. Amino acid decomposition increases with temperature alongside Maillard reaction products (Cho et al., 2019; Jeong et al., 2021). Lee J. H. (2018) has discussed that the Maillard reaction products level in red ginseng extracts typically increases with amino acid content. This is due to a simultaneous increase in the ionization constant of water ( $K_w$ ) at high temperatures (Lee et al., 2018).

Table 12. Yield of SWE hydrolysates from different parts of *K. pelamis*

Conditions	Hydrolysis efficiency (%)		
	HH	VH	SH
160°C	42.83±0.69 <sup>e</sup>	72.50±0.31 <sup>e</sup>	57.33±0.33 <sup>e</sup>
180°C	52.00±0.24 <sup>d</sup>	76.00±0.11 <sup>d</sup>	65.33±0.60 <sup>d</sup>
200°C	63.00±0.48 <sup>c</sup>	82.50±1.27 <sup>c</sup>	72.67±0.61 <sup>c</sup>
220°C	67.83±0.23 <sup>b</sup>	88.00±0.22 <sup>b</sup>	76.67±1.38 <sup>b</sup>
240°C	73.17±0.39 <sup>a</sup>	90.17±0.96 <sup>a</sup>	79.50±0.12 <sup>a</sup>

- Values are expressed as mean ± SD (n=3).
- Different letters indicate significant differences (p<0.05).
- HH, head hydrolysates of *K. pelamis*; VH, viscera hydrolysates of *K. pelamis*; SH, skin hydrolysates of *K. pelamis*.

Table 13. Maillard reaction products (MRPs) of SWE hydrolysates from different parts of *K. pelamis*

Conditions	MRPs (Abs 420 nm)		
	HH	VH	SH
160°C	0.085±0.001 <sup>e</sup>	0.194±0.002 <sup>c</sup>	0.083±0.027 <sup>d</sup>
180°C	0.140±0.004 <sup>d</sup>	0.263±0.002 <sup>b</sup>	0.172±0.004 <sup>c</sup>
200°C	0.177±0.002 <sup>c</sup>	0.375±0.006 <sup>a</sup>	0.195±0.002 <sup>b</sup>
220°C	0.200±0.001 <sup>b</sup>	0.397±0.026 <sup>a</sup>	0.197±0.003 <sup>b</sup>
240°C	0.247±0.003 <sup>a</sup>	0.372±0.013 <sup>a</sup>	0.222±0.117 <sup>a</sup>

- Values are expressed as mean ± SD (n=3).
- Different letters indicate significant differences (p<0.05).
- HH, head hydrolysates of *K. pelamis*; VH, viscera hydrolysates of *K. pelamis*; SH, skin hydrolysates of *K. pelamis*.

## 8. pH and color of *K. pelamis* hydrolysate

The pH levels of STH at varying temperatures are displayed in Table 14. The pH ranged from  $5.86 \pm 0.01$  to  $8.37 \pm 0.02$ , with the lowest value observed at HH and the highest at SH. As the temperature increased, the pH levels also increased, which can be explained by the promotion of the self-ionization process of water by subcritical water, resulting in an increase in  $[\text{OH}^-]$  groups (Park et al., 2022).

The color of hydrolyzed skipjack tuna at different temperatures is displayed in Table 15. As illustrated in Figure 8, the color of STH shifted from yellow to brown and darkened as the reaction temperature increased. As the hydrolysis process advanced, the L value decreased, while the redness index ( $a^*$ ) and  $b^*$  values increased. These results demonstrate an inverse correlation between the  $L^*$  value and the  $a^*$  value, supporting the theory that Maillard's response rises with increasing temperature (Delga-Andrade et al., 2010). The VH extract exhibited a distinctive color with a low  $L^*$  value and a high  $a^*$  value, unlike the extracts from other parts. This color variation is known to result from non-enzymatic browning reactions, including the Maillard reaction, due to an increase in temperature (Plaza et al., 2010).

Table 14. pH properties of SWE hydrolysates from different parts of *K. pelamis*

Conditions	pH		
	HH	VH	SH
160°C	5.86 ± 0.01 <sup>c</sup>	6.35 ± 0.02 <sup>d</sup>	6.32 ± 0.01 <sup>d</sup>
180°C	5.73 ± 0.02 <sup>d</sup>	6.31 ± 0.01 <sup>e</sup>	6.25 ± 0.01 <sup>e</sup>
200°C	5.75 ± 0.01 <sup>d</sup>	6.45 ± 0.01 <sup>c</sup>	6.36 ± 0.01 <sup>c</sup>
220°C	6.61 ± 0.01 <sup>b</sup>	7.16 ± 0.01 <sup>b</sup>	7.15 ± 0.01 <sup>b</sup>
240°C	7.91 ± 0.11 <sup>a</sup>	8.13 ± 0.01 <sup>a</sup>	8.37 ± 0.02 <sup>a</sup>

- Values are expressed as mean ± SD (n=3).
- Different letters indicate significant differences (p<0.05).
- HH, head hydrolysates of *K. pelamis*; VH, viscera hydrolysates of *K. pelamis*; SH, skin hydrolysates of *K. pelamis*.

Table 15. Color properties of SWE hydrolysates from different parts of *K. pelamis*

Conditions	HH			VH			SH		
	L*	a*	b*	L*	a*	b*	L*	a*	b*
160°C	53.83±0.64 <sup>a</sup>	-0.96±0.02 <sup>e</sup>	11.29±0.49 <sup>c</sup>	46.15±0.29 <sup>a</sup>	2.45±0.11 <sup>e</sup>	16.10±0.40 <sup>a</sup>	55.14±0.67 <sup>a</sup>	-0.61±0.02 <sup>e</sup>	7.46±0.06 <sup>d</sup>
180°C	49.69±1.04 <sup>b</sup>	0.71±0.04 <sup>d</sup>	14.79±0.77 <sup>b</sup>	40.74±0.12 <sup>b</sup>	4.50±0.07 <sup>d</sup>	11.92±0.23 <sup>b</sup>	50.43±0.18 <sup>b</sup>	0.29±0.03 <sup>d</sup>	11.27±0.16 <sup>c</sup>
200°C	46.26±0.23 <sup>c</sup>	3.32±0.05 <sup>c</sup>	15.87±0.32 <sup>b</sup>	38.69±0.19 <sup>c</sup>	5.18±0.08 <sup>c</sup>	9.20±0.03 <sup>d</sup>	46.20±0.39 <sup>c</sup>	2.20±0.04 <sup>c</sup>	13.92±0.17 <sup>b</sup>
220°C	46.00±0.26 <sup>c</sup>	4.44±0.05 <sup>b</sup>	17.71±0.29 <sup>a</sup>	38.01±0.80 <sup>c</sup>	5.88±0.25 <sup>b</sup>	7.52±0.40 <sup>e</sup>	46.78±0.11 <sup>c</sup>	3.59±0.06 <sup>a</sup>	17.24±0.40 <sup>a</sup>
240°C	43.41±0.19 <sup>d</sup>	5.14±0.34 <sup>a</sup>	14.38±1.53 <sup>b</sup>	40.17±0.20 <sup>b</sup>	7.36±0.05 <sup>a</sup>	11.32±0.15 <sup>c</sup>	44.10±0.88 <sup>d</sup>	3.05±0.41 <sup>b</sup>	15.90±2.34 <sup>a</sup>

– Values are expressed as mean ± SD (n=3).

– Different letters indicate significant differences (p<0.05).

– HH, head hydrolysates of *K. pelamis*; VH, viscera hydrolysates of *K. pelamis*; SH, skin hydrolysates of *K. pelamis*.

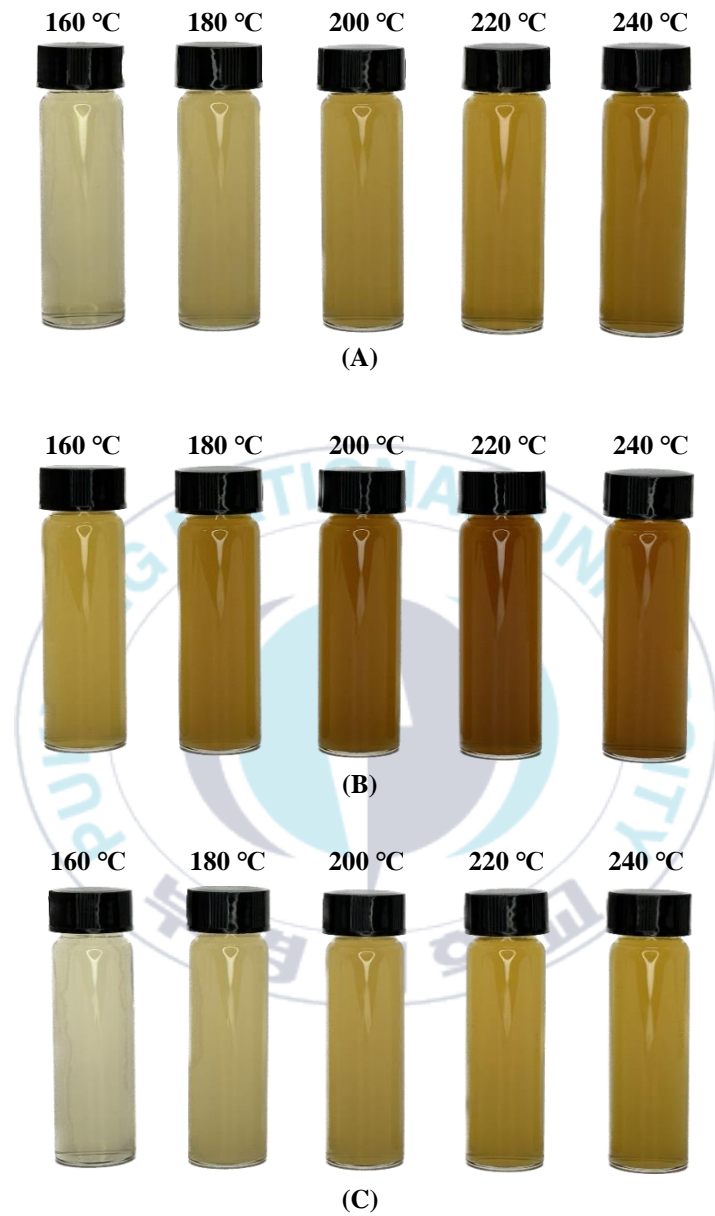


Figure 8. Visual appearance of SWE hydrolysates from different parts of *K. pelamis*.

- (A) Head hydrolysates of *K. pelamis*
- (B) Viscera hydrolysates of *K. pelamis*
- (C) Skin hydrolysates of *K. pelamis*

## 9. Total sugar and reducing sugar in *K. pelamis* hydrolysate

The sugar contents of STH are given in Table 16. Total sugar refers to the combination of reducing sugar and non-reducing sugar, and reducing sugar refers to sugar containing an aldehyde group that is oxidized to carboxylic acid. The total and reducing sugars varied depending on the hydrolysis temperature. The total amount of sugar decreased with the increase in temperature. For the HH, it went from  $6.44 \pm 0.22$  to  $13.34 \pm 0.67$  mg glucose/g, and for the VH and SH, it went from  $12.81 \pm 0.20$  to  $55.19 \pm 0.82$  mg glucose/g,  $6.34 \pm 0.11$  to  $13.69 \pm 0.49$  mg glucose/g. These findings are attributed to decreased sugar content resulting from the browning reaction or caramelization at high temperatures (Jang & Moon, 2005). The VH and SH showed peak values of  $23.62 \pm 2.04$  mg glucose/g and  $7.95 \pm 0.43$  mg glucose/g at 220°C. Meanwhile, for the HH, the maximum value of  $8.87 \pm 1.09$  mg glucose/g occurred at 200°C. However, after surpassing 200°C, the concentration decreased due to the conversion of reducing sugars into decomposition products (Mohan et al., 2015).

Table 16. Total sugar & reducing sugar contents of SWE hydrolysates from different parts of *K. pelamis*

Conditions	Total sugar (mg glucose/g)			Reducing sugar (mg glucose/g)		
	HH	VH	SH	HH	VH	SH
160°C	11.17±0.23 <sup>b</sup>	55.19±0.82 <sup>a</sup>	13.69±0.49 <sup>a</sup>	1.45±0.66 <sup>c</sup>	8.28±0.52 <sup>d</sup>	4.28±0.25 <sup>c</sup>
180°C	12.03±0.55 <sup>b</sup>	48.56±0.90 <sup>b</sup>	11.86±0.36 <sup>b</sup>	5.12±0.52 <sup>b</sup>	13.87±2.98 <sup>c</sup>	4.53±0.63 <sup>c</sup>
200°C	13.34±0.67 <sup>a</sup>	38.07±2.06 <sup>c</sup>	12.16±0.21 <sup>b</sup>	8.87±1.09 <sup>a</sup>	19.53±1.39 <sup>b</sup>	6.03±0.63 <sup>b</sup>
220°C	11.33±0.45 <sup>b</sup>	24.02±0.43 <sup>d</sup>	10.90±0.19 <sup>c</sup>	7.87±0.13 <sup>a</sup>	23.62±2.04 <sup>a</sup>	7.95±0.43 <sup>a</sup>
240°C	6.44±0.22 <sup>c</sup>	12.81±0.20 <sup>e</sup>	6.34±0.11 <sup>d</sup>	5.53±0.66 <sup>b</sup>	15.20±1.09 <sup>c</sup>	3.78±0.38 <sup>c</sup>

– Values are expressed as mean ± SD (n=3).

– Different letters indicate significant differences (p<0.05).

– HH, head hydrolysates of *K. pelamis*; VH, viscera hydrolysates of *K. pelamis*; SH, skin hydrolysates of *K. pelamis*.

## 10. Total protein content in *K. pelamis* hydrolysate

The protein content of STH at different temperatures is presented in Table 17. Changes in the relative dielectric constant impact the extraction and solubilization of proteins, resulting in increased solubility of proteins when the dielectric constant decreases. All three parts demonstrated the highest protein content at 200°C with values of  $219.86 \pm 2.26$  mg BSA/g,  $297.36 \pm 2.17$  mg BSA/g, and  $265.88 \pm 0.85$  mg BSA/g, respectively. However, the protein content gradually decreased after reaching 200°C. This is believed to occur due to the Maillard reaction between the sugar and the protein or thermal decomposition of the protein caused by the high subcritical water temperature for an extended period (Zhang et al., 2020). This is consistent with the findings of a prior study on oyster hydrolysate extraction using subcritical water (Lee et al., 2021).

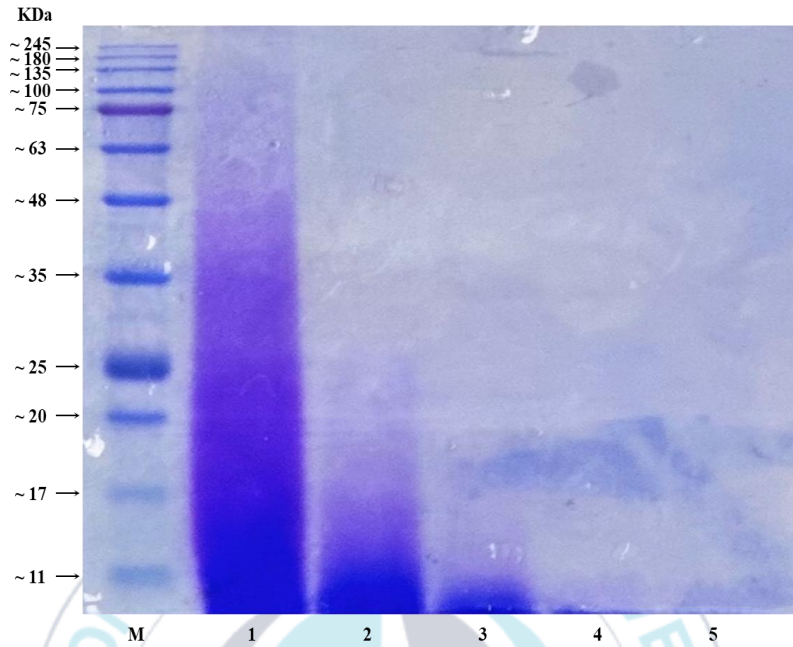
Table 17. Total protein contents of SWE hydrolysates from different parts of *K. pelamis*

Conditions	Total protein (mg BSA/g)		
	Head	Viscera	Skin
160°C	162.45 ± 0.89 <sup>e</sup>	262.18 ± 1.82 <sup>c</sup>	230.79 ± 0.32 <sup>d</sup>
180°C	199.77 ± 1.28 <sup>c</sup>	288.01 ± 2.22 <sup>b</sup>	248.01 ± 1.31 <sup>b</sup>
200°C	219.86 ± 2.26 <sup>a</sup>	297.36 ± 2.17 <sup>a</sup>	265.88 ± 0.85 <sup>a</sup>
220°C	202.73 ± 0.89 <sup>b</sup>	285.23 ± 1.67 <sup>b</sup>	239.49 ± 0.42 <sup>c</sup>
240°C	175.14 ± 1.25 <sup>d</sup>	261.34 ± 1.89 <sup>c</sup>	214.58 ± 0.16 <sup>e</sup>

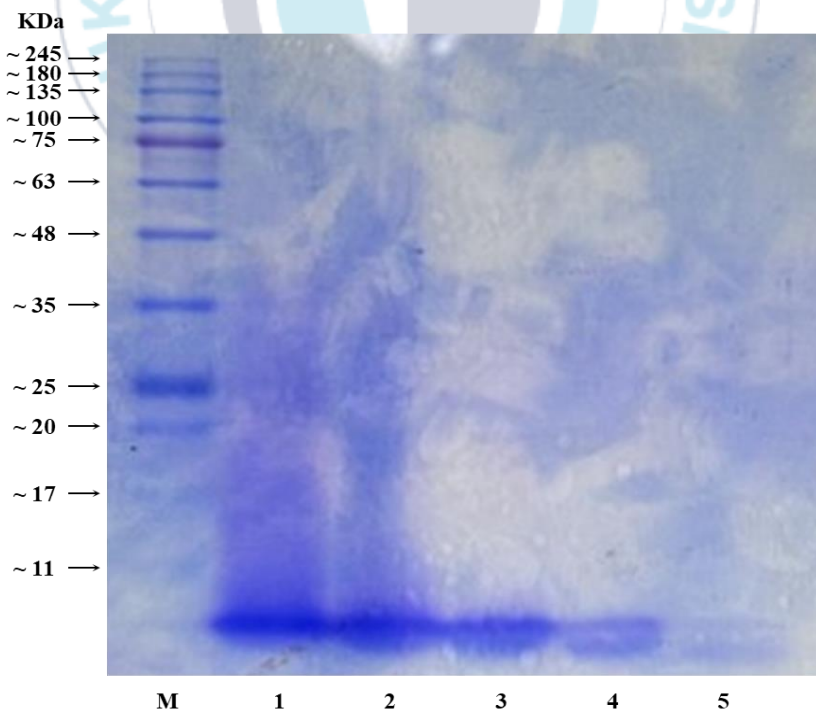
- Values are expressed as mean ± SD (n=3).
- Different letters indicate significant differences (p<0.05).
- HH, head hydrolysates of *K. pelamis*; VH, viscera hydrolysates of *K. pelamis*; SH, skin hydrolysates of *K. pelamis*.

## 11. SDS–PAGE of *K. pelamis* hydrolysate

The SDS–PAGE electrophoresis in Figure 9 illustrates the molecular weight pattern of STH at different temperatures. The protein of skip–jack tuna is decomposed through subcritical water hydrolysis, and the amount of reduction rises with increasing temperature. At 160°C, the HH generated a band of 75 KDa, while the VH produced a 35 KDa band, and the SH formed a 63 KDa band. This shows the highest molecular weight achieved. However, at a temperature of 180°C, the peptide bands decreased to 25 KDa, 11 KDa, and 25 KDa in the VH and SH, respectively. Most of the peptide bands disappeared at temperatures above that and became low–molecular–weight, except for the 11 KDa band identified in the HH. This might be attributed to the decay of low molecular weight peptides caused by the relatively high temperature (Ramachandraiah et al., 2017). Thus, subcritical water temperature conditions may reduce the molecular weight of STH. The average size of peptides in hydrolysates is crucial in determining functional activity, with numerous bioactive peptides weighing less than 1 KDa already reported (Ahmed & Chun, 2018).



(A)



(B)

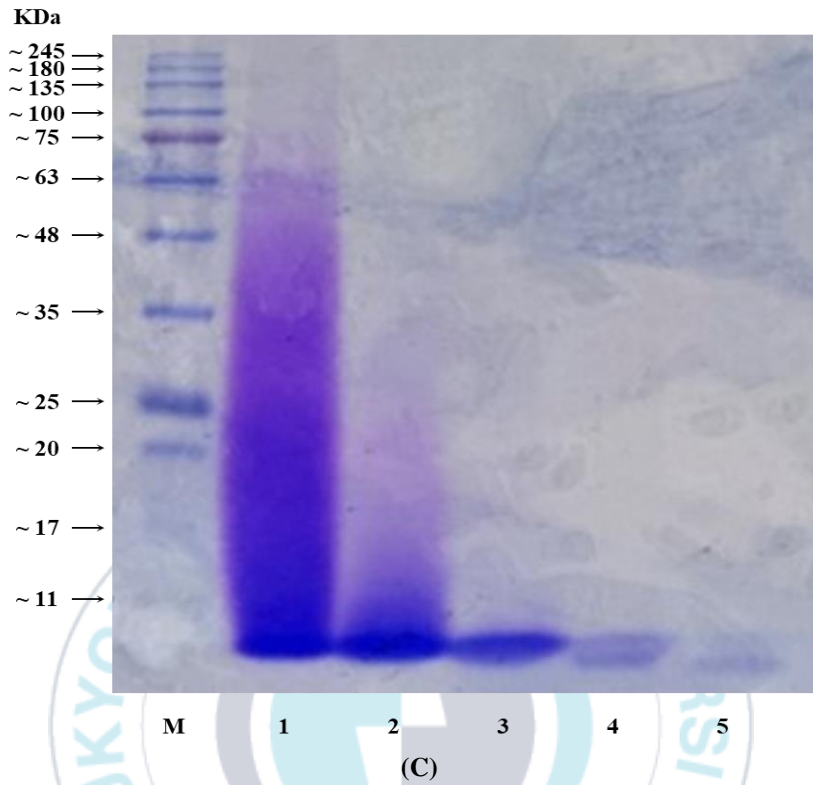


Figure 9. SDS-PAGE pattern of SWE hydrolysates from different conditions of *K. pelamis*.

(A) Head hydrolysates of *K. pelamis*

(B) Viscera hydrolysates of *K. pelamis*

(C) Skin hydrolysates of *K. pelamis*

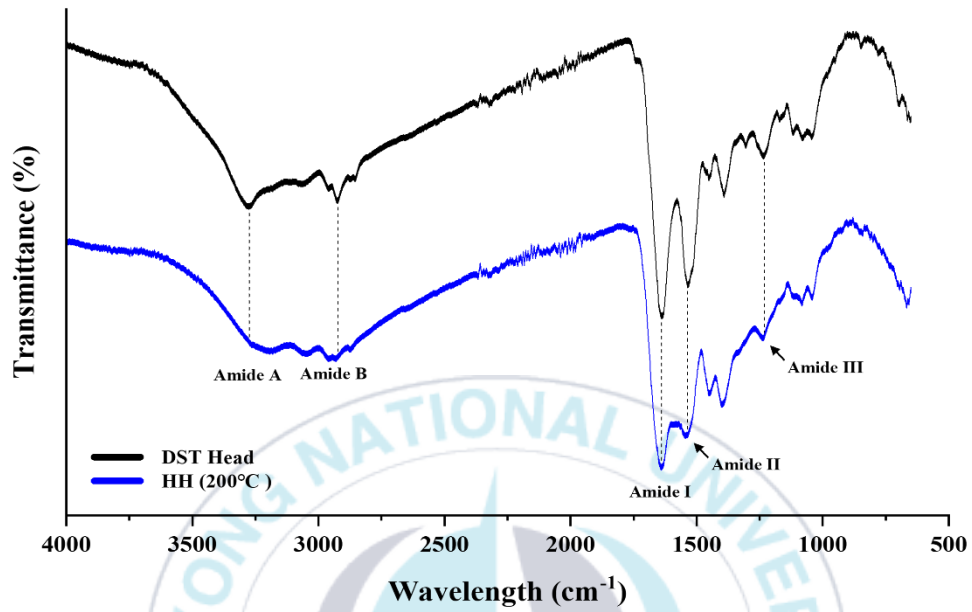
M: Marker; 1-5: hydrolysates at 160, 180, 200, 220, 240 °C.

## 12. FT-IR spectrum of *K. pelamis* hydrolysate

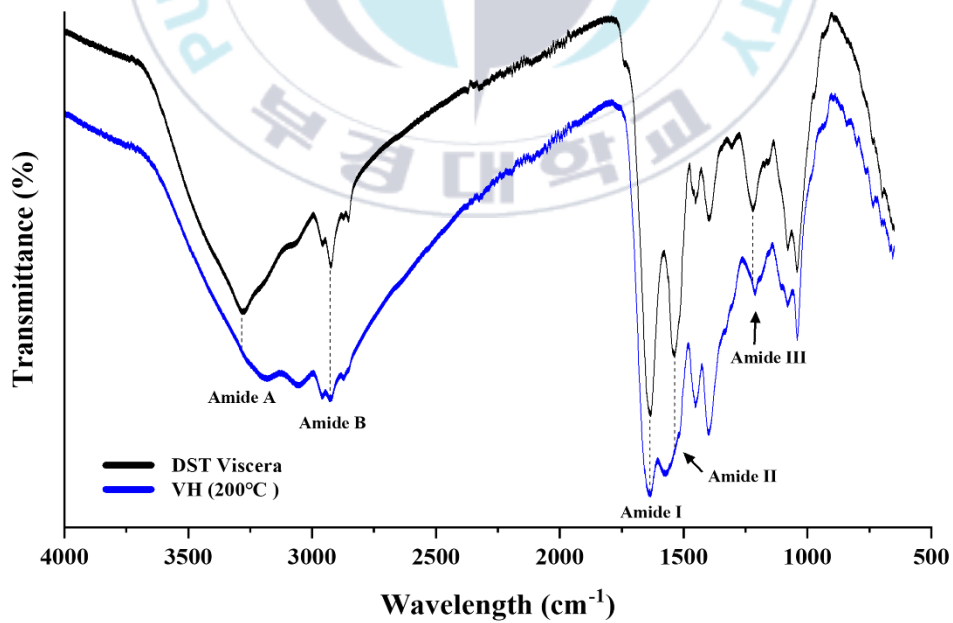
FT-IR spectral analysis was conducted using a freeze-dried sample of the STH that was extracted at 200°C, the temperature at which the previous results showed the highest total protein content. The analysis compared the STH sample with the DST, and the resulting FTIR spectrum is presented in Figure 10. The presence of amide A and B bands, as well as amide I, II, and III peaks, was confirmed in all regions. The amide A band typically corresponds to the free NH stretching, while stretching vibrations occur within the range of 3400–3440 cm<sup>-1</sup>. When involved in hydrogen bonding, the NH group of the peptide typically experiences a shift towards a lower frequency, reaching roughly 3300 cm<sup>-1</sup> (Doyle et al., 1975). In every region, the amide bands were identified at 3280 cm<sup>-1</sup>, 3270 cm<sup>-1</sup>, and 3282 cm<sup>-1</sup>. Meanwhile, the Amide B band occurs in the asymmetric stretching of CH<sub>2</sub>, noted at 2925 cm<sup>-1</sup>, 2925 cm<sup>-1</sup>, and 2927 cm<sup>-1</sup> per region. These results coincide with the analysis of collagen obtained from bigeye tuna by Ahmed R. (2019) (Ahmed et al., 2019). Amide I stretching occurs mainly due to C=O (carbonyl) vibrations within the spectral range of 1600–1660 cm<sup>-1</sup>, while amide II stretching appears at approximately 1550 cm<sup>-1</sup> and is attributed to N-H and C-N stretching. Similarly, amide III stretching arises mainly due to C-N stretching and N-H vibrations, and C-H banding can also be seen at these frequencies (Asaduzzaman et al., 2020; Muyonga et al., 2004). For the head, the respective bands were observed at 1639 cm<sup>-1</sup>, 1544 cm<sup>-1</sup>, and 1236 cm<sup>-1</sup>; for the viscera, the frequencies were 1639 cm<sup>-1</sup>, 1535 cm<sup>-1</sup>, and 1238 cm<sup>-1</sup>; and for the skin, they were 1639 cm<sup>-1</sup>, 1538 cm<sup>-1</sup>, and 1234 cm<sup>-1</sup>. For the

head, the respective bands were observed at  $1639\text{ cm}^{-1}$ ,  $1544\text{ cm}^{-1}$ , and  $1236\text{ cm}^{-1}$ ; for the viscera, the frequencies were  $1639\text{ cm}^{-1}$ ,  $1535\text{ cm}^{-1}$ , and  $1238\text{ cm}^{-1}$ ; and for the skin, they were  $1639\text{ cm}^{-1}$ ,  $1538\text{ cm}^{-1}$ , and  $1234\text{ cm}^{-1}$ . All bands were recorded in terms of  $\text{cm}^{-1}$ . After the hydrolysis process, slight differences in the width and depth of the spectrum are noticeable. This allows for identification of the structural disparities between STH and DST, as well as characterization of the compounds.





(A)



(B)

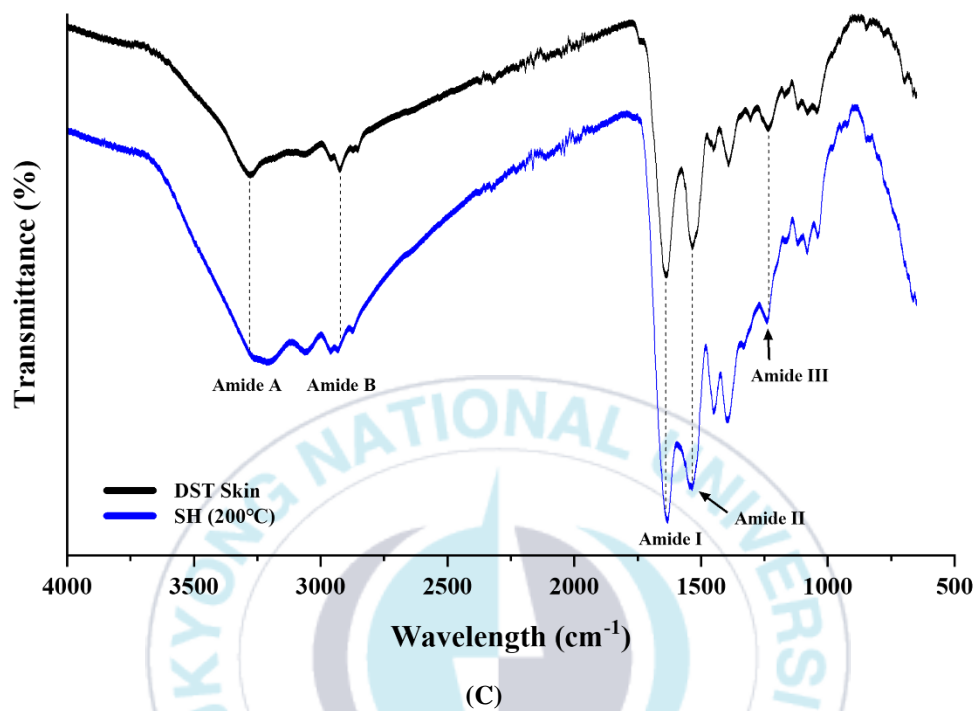


Figure 10. Infrared absorption properties of *K. pelamis* by FT-IR Analysis.

(A) Head hydrolysates and de-oiled raw sample of *K. pelamis*; (B) Viscera hydrolysates and de-oiled raw sample of *K. pelamis*; (C) Skin hydrolysates and de-oiled raw sample of *K. pelamis*.

### 13. Amino acid analysis of *K. pelamis* hydrolysate

Amino acid analysis used a freeze-dried sample of the STH extracted at a temperature of 200°C, which had the highest total protein content in the previous results. The DST was then compared to this. The total amino acid content for DST was 450.14%, 443.73%, and 633.63%, respectively. The total amino acid content for STH was 484.63%, 537.58%, and 588.82%. Dominant contents of leucine, glutamic acid, glycine, arginine, and alanine were noted among them, as shown in Table 18. The free amino acid content of the DST was 13.96%, 33.72%, and 45.83%, respectively, while for the STH, it was 39.56%, 47.10%, and 26.24%, with histidine and taurine as the dominant constituents. Free amino acid content is shown in Table 19. However, each part exhibited differences in composition and content. These results align with those of a previous study that used collagen extracted from tuna skin (Ahmed & Chun, 2018). Glutamic acid is a significant group of neurotransmitters under investigation for enhancing the effectiveness of anticancer drugs (Dutta et al., 2013). Further research has revealed that glycine, as a neurotransmission inhibitor, may prove useful in treating ailments such as sepsis, arthritis, and inflammatory diseases (Wheeler et al., 1999). Taurine is currently being examined for its protective capabilities, such as membrane stabilization, detoxification, antioxidant properties, calcium homeostasis, glycolysis, and glycogenesis (Stapleton, 1997). Subcritical water has the ability to dissolve less soluble molecules at increasing temperatures due to the temperature dependence of the dielectric constant. Therefore, the content of amino acids with low molecular weight, like glycine or alanine, tended to in-

crease as they underwent hydrolysis at 200°C. However, there was a decreasing pattern in thermosensitive and high molecular weight amino acids at high temperatures. Additionally, the tendency to increase or decrease depending on hydrolysis was found to be slightly different for each site, and further research is required to ascertain the underlying mechanism (Ziero et al., 2022).



Table 18. Constituent amino acids profiles of SWE hydrolysates from different parts of *K. pelamis*

Amino Acid Compositions mg/g (%)	Constituent amino acid					
	Raw sample			200°C hydrolysates		
	Head	Viscera	Skin	HH	VH	SH
Essential Amino Acid (EAA)						
Histidine	15.48 (3.44)	12.82 (2.89)	34.57 (5.46)	20.81 (4.29)	14.83 (2.76)	30.38 (5.16)
Threonine	27.63 (6.14)	33.03 (7.44)	35.90 (5.67)	22.22 (4.58)	25.01 (4.65)	29.72 (5.05)
Valine	21.06 (4.68)	28.62 (6.45)	29.51 (4.66)	24.86 (5.13)	35.72 (6.64)	29.47 (5.01)
Methionine	N.D.	N.D.	N.D.	N.D.	N.D.	N.D.
Tryptophan	N.D.	N.D.	N.D.	N.D.	N.D.	N.D.
Phenylalanine	20.84 (4.63)	23.79 (5.36)	23.81 (3.76)	20.75 (4.28)	24.72 (4.60)	23.06 (3.92)
Isoleucine	18.16 (4.03)	23.91 (5.39)	23.68 (3.74)	21.66 (4.47)	27.99 (5.21)	23.01 (3.91)
Leucine	33.49 (7.44)	42.06 (9.48)	41.46 (6.54)	36.48 (7.53)	46.68 (8.68)	41.17 (6.99)
Lysine	18.59 (4.13)	23.31 (5.25)	40.28 (6.36)	22.17 (4.57)	32.35 (6.02)	30.48 (5.18)
<b>Total</b>	<b>155.24 (34.49)</b>	<b>187.54 (42.26)</b>	<b>229.22 (36.19)</b>	<b>168.95 (34.85)</b>	<b>207.30 (38.56)</b>	<b>207.29 (35.22)</b>
Non-Essential Amino Acid (NEAA)						
Aspartic acid	29.75 (6.61)	32.77 (7.39)	45.44 (7.17)	19.95 (4.12)	21.30 (3.96)	21.53 (3.66)
Glutamic acid	61.38 (13.64)	62.25 (14.03)	85.36 (13.47)	78.25 (16.15)	95.72 (17.80)	91.97 (15.62)
Asparagine	N.D.	N.D.	N.D.	N.D.	N.D.	N.D.
Serine	18.56 (4.12)	20.14 (4.54)	24.15 (3.81)	16.35 (3.37)	20.60 (3.83)	19.11 (3.25)
Glutamine	N.D.	N.D.	N.D.	N.D.	N.D.	N.D.
Glycine	71.73 (15.94)	26.21 (5.91)	85.39 (13.48)	68.07 (14.04)	41.83 (7.78)	88.73 (15.07)
Citrulline	N.D.	N.D.	N.D.	N.D.	N.D.	N.D.
Arginine	45.78 (10.17)	40.48 (9.12)	54.16 (8.55)	39.22 (8.09)	38.23 (7.11)	49.48 (8.40)
Alanine	46.28 (10.28)	33.04 (7.45)	55.81 (8.81)	47.76 (9.86)	46.53 (8.66)	57.45 (9.76)
Taurine	5.67 (1.26)	18.47 (4.16)	4.03 (0.64)	7.94 (1.64)	29.50 (5.49)	4.49 (0.76)
GABA	N.D.	N.D.	N.D.	N.D.	N.D.	N.D.
Tyrosine	N.D.	14.09 (3.18)	N.D.	N.D.	7.56 (1.41)	N.D.
Ornithine	N.D.	N.D.	N.D.	N.D.	N.D.	N.D.
Proline	15.75 (3.50)	8.74 (1.97)	50.08 (7.90)	38.13 (7.87)	29.02 (5.40)	48.78 (8.28)
<b>Total</b>	<b>294.90 (65.51)</b>	<b>256.19 (57.74)</b>	<b>404.42 (63.81)</b>	<b>315.68 (65.15)</b>	<b>330.27 (61.44)</b>	<b>381.53 (64.78)</b>
<b>EAA + NEAA</b>	<b>450.14</b>	<b>443.73</b>	<b>633.63</b>	<b>484.63</b>	<b>537.58</b>	<b>588.82</b>

– N.D.: Not detected.

– HH, head hydrolysates of *K. pelamis*; VH, viscera hydrolysates of *K. pelamis*; SH, skin hydrolysates of *K. pelamis*.

Table 19. Free amino acids profiles of SWE hydrolysates from different parts of *K. pelamis*

Amino Acid Compositions mg/g (%)	Free amino acid					
	Raw sample			200°C hydrolysates		
	Head	Viscera	Skin	HH	VH	SH
Essential Amino Acid (EAA)						
Histidine	6.16 (44.10)	0.12 (0.34)	13.51 (29.48)	8.05 (20.33)	0.92 (1.95)	18.04 (68.75)
Threonine	0.18 (1.28)	0.56 (1.65)	0.70 (1.53)	0.75 (1.89)	2.01 (4.26)	0.17 (0.66)
Valine	0.16 (1.16)	1.09 (3.24)	0.82 (1.78)	0.79 (2.00)	1.72 (3.66)	0.37 (1.41)
Methionine	0.02 (0.12)	0.53 (1.58)	0.57 (1.23)	0.47 (1.19)	0.32 (0.68)	0.07 (0.25)
Tryptophan	N.D.	N.D.	N.D.	N.D.	0.28 (0.59)	0.04 (0.14)
Phenylalanine	0.07 (0.51)	1.23 (3.63)	0.83 (1.80)	0.82 (2.06)	1.26 (2.68)	0.11 (0.40)
Isoleucine	0.09 (0.66)	0.87 (2.58)	0.62 (1.36)	0.58 (1.47)	1.29 (2.73)	0.22 (0.83)
Leucine	0.19 (1.39)	2.59 (7.69)	1.88 (4.09)	1.79 (4.51)	2.50 (5.30)	0.47 (1.77)
Lysine	0.37 (2.65)	2.28 (6.76)	2.20 (4.81)	1.73 (4.37)	1.98 (4.21)	0.92 (3.50)
<b>Total</b>	<b>7.24 (51.87)</b>	<b>9.27 (27.47)</b>	<b>21.12 (44.30)</b>	<b>14.97 (37.82)</b>	<b>12.28 (26.06)</b>	<b>20.39 (77.71)</b>
Non-Essential Amino Acid (NEAA)						
Aspartic acid	0.04 (0.27)	0.97 (2.89)	3.71 (8.09)	5.23 (13.22)	1.30 (2.77)	0.06 (0.21)
Glutamic acid	0.32 (2.30)	0.08 (0.24)	0.16 (0.36)	0.17 (0.45)	4.28 (9.08)	0.31 (1.19)
Asparagine	0.004 (0.03)	0.03 (0.07)	0.11 (0.25)	0.10 (0.25)	0.12 (0.25)	0.004 (0.02)
Serine	0.09 (0.63)	1.49 (4.41)	1.52 (3.32)	1.40 (3.54)	1.48 (3.14)	0.13 (0.51)
Glutamine	0.64 (4.57)	0.01 (0.03)	0.02 (0.04)	0.01 (0.03)	2.49 (5.29)	0.50 (1.89)
Glycine	0.15 (1.08)	2.16 (6.41)	5.85 (12.77)	4.04 (10.20)	1.42 (3.01)	0.17 (0.63)
Citrulline	N.D.	N.D.	N.D.	N.D.	0.18 (0.38)	N.D.
Arginine	0.12 (0.87)	3.46 (10.26)	1.72 (3.76)	1.46 (3.69)	1.66 (3.53)	0.12 (0.45)
Alanine	0.55 (3.91)	3.91 (11.61)	3.79 (8.28)	3.36 (8.48)	4.56 (9.67)	0.69 (2.62)
Taurine	4.43 (31.74)	8.74 (25.91)	3.86 (8.43)	5.93 (15.00)	15.00 (31.82)	3.43 (13.08)
GABA	0.02 (0.15)	0.04 (0.12)	0.08 (0.17)	0.05 (0.11)	0.07 (0.14)	0.04 (0.14)
Tyrosine	0.08 (0.59)	1.13 (3.36)	0.87 (1.89)	0.71 (1.79)	1.22 (2.59)	0.13 (0.49)
Ornithine	0.04 (0.31)	0.96 (2.85)	2.16 (4.71)	1.27 (3.20)	0.14 (0.30)	0.10 (0.40)
Proline	0.24 (1.69)	1.47 (4.36)	0.85 (1.86)	0.88 (2.22)	0.91 (1.93)	0.17 (0.66)
<b>Total</b>	<b>6.72 (44.8.13)</b>	<b>24.45 (72.53)</b>	<b>24.71 (55.70)</b>	<b>24.60 (62.18)</b>	<b>34.82 (73.94)</b>	<b>5.85 (22.29)</b>
<b>EAA + NEAA</b>	<b>13.96</b>	<b>33.72</b>	<b>45.83</b>	<b>39.56</b>	<b>47.10</b>	<b>26.24</b>

– N.D.: Not detected.

– HH, head hydrolysates of *K. pelamis*; VH, viscera hydrolysates of *K. pelamis*; SH, skin hydrolysates of *K. pelamis*.

#### 14. Antioxidant activities of *K. pelamis* hydrolysate (DPPH, ABTS<sup>+</sup>, FRAP)

The antioxidant activity of STH was assessed utilizing DPPH radical scavenging, ABTS<sup>+</sup> radical scavenging, and FRAP assays. Table 20 presents the results obtained. The DPPH radical scavenging approach is based on the antioxidant's ability to donate hydrogen atoms and is commonly employed in the evaluation of the radical scavenging capacity of natural compounds (Hao et al., 2019). The highest DPPH radical scavenging ability was observed in HH, VH, and SH,  $9.50 \pm 0.06$  mg TE/g,  $15.45 \pm 0.10$  mg TE/g, and  $10.71 \pm 0.39$  mg TE/g. ABTS<sup>+</sup> radical scavenging activity is determined using the decolorization process, which involves antioxidants reacting with cationic free radical hydrogen-donating antioxidants to measure their antioxidant activity (Jeong et al., 2021). The results of ABTS<sup>+</sup> radical scavenging ability exhibited a similar pattern to the DPPH radical scavenging ability results. The highest values of  $52.21 \pm 1.05$  mg TE/g,  $80.30 \pm 1.70$  mg TE/g, and  $68.28 \pm 7.19$  mg TE/g were observed in the 240°C HH, VH, and SH, indicating high activity. FRAP, which determines the antioxidant's ability to donate electrons or hydrogen by reducing Fe<sup>3+</sup> to Fe<sup>2+</sup>, was also used for measurement purposes (Je et al., 2015). Higher activity was observed as the temperature increased, as evidenced by the previous ABTS<sup>+</sup> and DPPH radical scavenging activity results. These results were attributed in a previous study to the decrease in the dielectric constant of subcritical water, resulting in increased antioxidant extraction efficiency (Park et al., 2022). Furthermore, alterations in the quantity and makeup of unbound amino acids and small peptides

during hydrolysis seem to have a correlation with the antioxidant capability of mackerel hydrolysate (Sila & Bougatef, 2016).



Table 20. Antioxidant activities of SWE hydrolysates from different parts of *K. pelamis*

Conditions	Antioxidant activities								
	ABTS <sup>+</sup> radical scavenging (mg TE/g)			DPPH radical scavenging (mg TE/g)			FRAP assays (mg TE/g)		
	HH	VH	SH	HH	VH	SH	HH	VH	SH
160°C	11.14±1.22 <sup>e</sup>	33.58±3.51 <sup>e</sup>	18.82±5.60 <sup>e</sup>	2.36±0.66 <sup>e</sup>	5.89±0.14 <sup>e</sup>	2.06±1.68 <sup>d</sup>	0.67±0.04 <sup>e</sup>	3.28±0.05 <sup>e</sup>	2.48±0.03 <sup>e</sup>
180°C	19.47±0.10 <sup>d</sup>	42.68±3.53 <sup>d</sup>	28.22±2.50 <sup>d</sup>	3.92±0.23 <sup>d</sup>	8.58±0.27 <sup>d</sup>	4.93±0.15 <sup>c</sup>	1.95±0.11 <sup>d</sup>	5.3±0.09 <sup>d</sup>	3.37±0.01 <sup>d</sup>
200°C	29.89±2.30 <sup>c</sup>	52.39±3.59 <sup>c</sup>	37.63±2.85 <sup>c</sup>	6.52±0.06 <sup>c</sup>	11.58±0.07 <sup>c</sup>	8.14±0.10 <sup>b</sup>	3.62±0.11 <sup>c</sup>	8.57±0.09 <sup>c</sup>	4.47±0.08 <sup>c</sup>
220°C	37.68±1.70 <sup>b</sup>	65.07±0.72 <sup>b</sup>	48.28±2.75 <sup>b</sup>	8.77±0.17 <sup>b</sup>	14.88±0.38 <sup>b</sup>	9.95±0.30 <sup>a</sup>	5.42±0.16 <sup>b</sup>	12.00±0.16 <sup>b</sup>	5.31±0.14 <sup>b</sup>
240°C	52.21±1.05 <sup>a</sup>	80.30±1.70 <sup>a</sup>	68.28±7.19 <sup>a</sup>	9.50±0.06 <sup>a</sup>	15.45±0.10 <sup>a</sup>	10.71±0.39 <sup>a</sup>	6.24±0.21 <sup>a</sup>	12.71±0.30 <sup>a</sup>	6.34±0.20 <sup>a</sup>

– Values are expressed as mean ± SD (n=3).

– Different letters indicate significant differences (p<0.05).

– HH, head hydrolysates of *K. pelamis*; VH, viscera hydrolysates of *K. pelamis*; SH, skin hydrolysates of *K. pelamis*.

## 15. Antidiabetic activity of *K. pelamis* hydrolysate

$\alpha$ -Glucosidase is an enzyme that catalyzes the hydrolysis of polysaccharides like  $\alpha$ -glucose. Limiting these enzymes can help regulate the postprandial blood sugar surge. Our study measured the  $\alpha$ -glucosidase inhibitory activity of STH. Table 21 demonstrates STH's inhibitory activity by various temperatures and sections. As the temperature increased, the activity levels of the HH, VH, and SH increased. Specifically, the activity of the HH increased from  $17.92\% \pm 1.60\%$  to  $73.83\% \pm 0.92\%$ , the activity of the VH increased from  $27.52\% \pm 0.80\%$  to  $93.47\% \pm 0.68\%$ , and the SH increased from  $2.09\% \pm 1.60\%$  to  $79.68\% \pm 0.49\%$ . It was observed that the VH exhibited superior inhibitory activity compared to other parts even at  $160^\circ\text{C}$ , with an activity level of  $27.52\% \pm 0.80\%$ . Table 22 presents a comparison of the  $\text{IC}_{50}$  values of inhibitory activity for the most active temperature condition of  $240^\circ\text{C}$ . The  $\alpha$ -glucosidase inhibition rate was highest in the VH, with values of  $6.38 \pm 0.09$  mg/mL,  $2.08 \pm 0.17$  mg/mL, and  $5.18 \pm 0.14$  mg/mL. Further research is necessary to comprehend the mechanism of antidiabetic activity with regards to temperature change and location.

Table 21.  $\alpha$ -Glucosidase inhibitory activity of *K. pelamis* de-oiled hydrolysates obtained at different conditions.

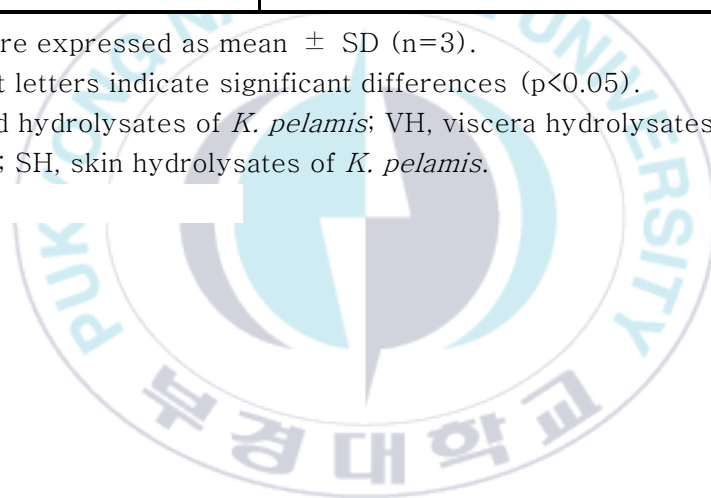
Conditions	$\alpha$ -Glucosidase Inhibitory Activity (%)			Acarbose
	HH	VH	SH	
160 °C	17.92±1.60 <sup>d</sup>	27.52±0.80 <sup>d</sup>	2.09±1.60 <sup>e</sup>	97.91±0.15
180 °C	29.13±0.49 <sup>d</sup>	42.43±0.18 <sup>d</sup>	24.88±2.28 <sup>d</sup>	
200 °C	40.83±2.96 <sup>c</sup>	60.10±1.85 <sup>c</sup>	46.43±0.68 <sup>c</sup>	
220 °C	54.68±0.01 <sup>b</sup>	79.93±0.62 <sup>b</sup>	62.99±0.62 <sup>b</sup>	
240 °C	73.83±0.92 <sup>a</sup>	93.47±0.68 <sup>a</sup>	79.68±0.49 <sup>a</sup>	

- Values are expressed as mean  $\pm$  SD (n=3).
- Different letters indicate significant differences (p<0.05).
- HH, head hydrolysates of *K. pelamis*; VH, viscera hydrolysates of *K. pelamis*; SH, skin hydrolysates of *K. pelamis*.

Table 22. IC<sub>50</sub> values of  $\alpha$ -glucosidase inhibitory activity of *K. pelamis* hydrolysate extracted at 240°C.

$\alpha$ -Glucosidase Inhibitory Activity	IC <sub>50</sub> value
HH (mg/mL)	6.38 ± 0.09 <sup>a</sup>
VH (mg/mL)	2.08 ± 0.17 <sup>c</sup>
SH (mg/mL)	5.18 ± 0.14 <sup>b</sup>
Acarbose ( $\mu$ g/mL)	0.02 ± 0.00001

- Values are expressed as mean  $\pm$  SD (n=3).
- Different letters indicate significant differences (p<0.05).
- HH, head hydrolysates of *K. pelamis*; VH, viscera hydrolysates of *K. pelamis*; SH, skin hydrolysates of *K. pelamis*.



## 16. Analysis of in vitro anti-inflammatory activity *K. pelamis* hydrolysate

Oxidative stress arises from an imbalance between free radical production and the antioxidant defense system, potentially leading to inflammation (Murugan & Parimelazhagan, 2014). Chronic inflammation is associated with aging-related diseases such as vascular disease, cancer, diabetes, dementia, and obesity (Hernandez-Ledesma et al., 2014). Inflammatory responses can result in increased vascular permeability, protein denaturation, membrane deformation, and the over-activation of phagocytes, leading to free radical generation (Umapathy, E. et al., 2010). Autoantigens may be produced in inflammatory diseases due to in vivo protein denaturation. Since agents that inhibit protein denaturation may have anti-inflammatory effects, in vitro protein denaturation assays are often employed in preliminary screening of potential anti-inflammatory drugs (Chamika W. A. S., et al 2021). Non-steroidal anti-inflammatory drugs (NSAIDs), comprising approximately 50 distinct types, are currently the most commonly prescribed treatments for inflammation (Vonkeman H. E. & van de Laar M. A., 2010). However, pharmaceuticals can be associated with various side effects. Therefore, evaluating the anti-inflammatory properties of natural substances is an important research objective. This study employs the protein denaturation method to assess the in vitro anti-inflammatory benefits of STH. Table 23 displays the results of protein denaturation inhibition analysis for *K. pelamis* de-oiled hydrolysates obtained under different conditions. Diclofenac sodium (1%, w/v), used as a standard drug, demonstrated an activity rate of  $92.15\% \pm 0.23\%$ .

Significant variations in STH activity were observed across different each part. The activity range of HH ranged from  $1.44\% \pm 0.03\%$  to  $16.30\% \pm 0.53\%$ , while VH exhibited a higher activity range of  $11.31\% \pm 0.48\%$  to  $20.52\% \pm 0.09\%$ . SH displayed an activity range between  $1.88\% \pm 0.49\%$  and  $10.35\% \pm 0.96\%$ , with  $240^{\circ}\text{C}$  showing maximum activity in all parts. Although there were slight differences in trends by parts, it can be observed that the viscera extract exhibited the most outstanding activity.



Table 23. Analysis of protein denaturation inhibition of *K. pelamis* de-oiled hydrolysates obtained at different conditions.

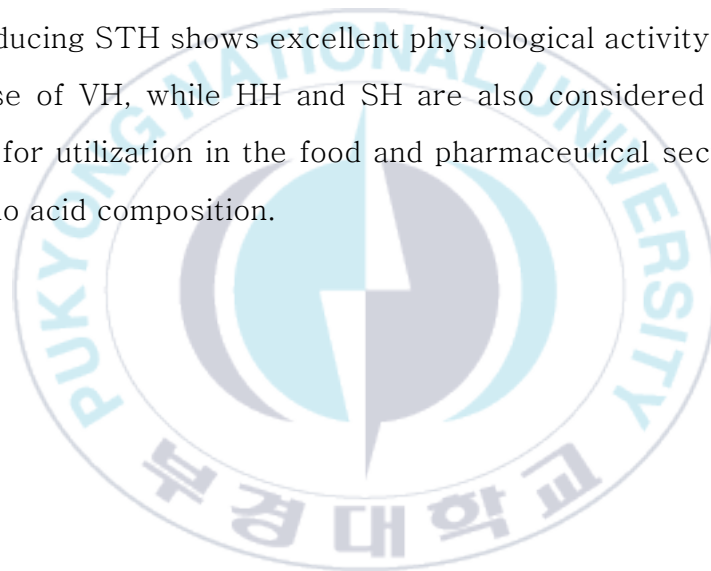
Conditions	Protein denaturation inhibition (%)		
	HH	VH	SH
160°C	1.44±0.23 <sup>c</sup>	11.31±0.48 <sup>e</sup>	5.28±0.51 <sup>c</sup>
180°C	6.88±0.18 <sup>b</sup>	15.63±0.29 <sup>c</sup>	1.88±0.49 <sup>d</sup>
200°C	6.72±0.18 <sup>b</sup>	20.52±0.09 <sup>a</sup>	4.64±0.26 <sup>c</sup>
220°C	6.98±0.55 <sup>b</sup>	14.09±0.46 <sup>d</sup>	9.04±0.39 <sup>b</sup>
240°C	16.30±0.53 <sup>a</sup>	17.80±0.31 <sup>b</sup>	10.35±0.96 <sup>a</sup>
Diclofenac sodium	92.15±0.03		

- Values are expressed as mean ± SD (n=3).
- Different letters indicate significant differences (p<0.05).
- HH, head hydrolysates of *K. pelamis*; VH, viscera hydrolysates of *K. pelamis*; SH, skin hydrolysates of *K. pelamis*.

## IV. Conclusion

In this study, lipids and proteins were extracted from skipjack tuna by-products using clean process technologies, including SC-CO<sub>2</sub> and SWH, and then evaluated for physicochemical and physiological activity. The extracted lipids (oil and PLs) underwent comprehensive analyses, including yield and purity, PLs composition, color, fatty acid composition, fat-soluble vitamin content, and TGA. Notably, the SO yield was more than twice as high as that of HO and VO. The net PL yield, considering applied purity, was highest at 3.24% from the head and lowest at 1.68% from the SP. The analysis confirmed that skipjack tuna PLs consist of PC, LPC, and PE, with a small amount of CD found in the skin. All extracted oils contained substantial amounts of  $\omega$ -3 unsaturated fatty acids, with the highest content observed in lipids extracted from the skin.  $\omega$ -3 was also detected in PLs, indicating their distinction as MPLs. Retinol was exclusively found in VO, while both oil and PLs from all parts contained high amounts of tocopherol. Furthermore, the TGA results established that the oil extracted through SC-CO<sub>2</sub> exhibited thermal stability, providing valuable data for future research. The STH obtained through SWH was analyzed for yield, color, MRPs, total sugar, reducing sugar, and total protein content. The SDS-PAGE and amino acid composition analyses revealed changes in protein content and composition at different temperatures. The physiological activities, including antioxidant, anti-diabetic, and anti-hypertensive, were evaluated. The hydrolysate exhibited an increasing yield with rising temperature, with the VH yielding the highest amount. The VH also showed the highest levels of total sugar and reducing sugar contents. The total

protein content exhibited a decreasing trend from 200°C, and the SDS-PAGE results showing that most protein bands became low molecular weight above 200°C. The amino acid composition of the 200°C extract contains the largest amounts of leucine, glutamic acid, glycine, arginine, and alanine. Additionally, histidine and taurine were identified as the highest free amino acids. The VH exhibited particularly elevated activity levels compared to other parts, showcasing superior antidiabetic and anti-inflammatory activities. Therefore, the use of subcritical water in producing STH shows excellent physiological activity, especially in the case of VH, while HH and SH are also considered viable raw materials for utilization in the food and pharmaceutical sectors due to their amino acid composition.



## Reference

- Abuine, R., Rathnayake, A. U., & Byun, H. G. (2019). Biological activity of peptides purified from fish skin hydrolysates. *Fisheries and aquatic sciences*, *22*(1), 1–14.
- Afonso, C., Bandarra, N. M., Nunes, L., & Cardoso, C. (2016). Tocopherols in seafood and aquaculture products. *Critical reviews in food science and nutrition*, *56*(1), 128–140.
- Ahmmed, M. K., Ahmmed, F., Stewart, I., Carne, A., Tian, H. S., & Bekhit, A. E. D. A. (2021a). Omega–3 phospholipids in Pacific blue mackerel (*Scomber australasicus*) processing by–products. *Food Chemistry*, *353*, 129451.
- Ahmmed, M. K., Carne, A., Ahmmed, F., Stewart, I., Tian, H. S., & Bekhit, A. E. D. A. (2021b). Positional distribution of fatty acids and phospholipid composition in King salmon (*Oncorhynchus tshawytscha*) head, roe and skin using nuclear magnetic resonance spectroscopy. *Food Chemistry*, *363*, 130302.
- Ahmed, R., & Chun, B. S. (2018). Subcritical water hydrolysis for the production of bioactive peptides from tuna skin collagen. *The Journal of Supercritical Fluids*, *141*, 88–96.
- Ahmed, R., Haq, M., & Chun, B. S. (2019). Characterization of marine derived collagen extracted from the by–products of bigeye tuna (*Thunnus obesus*). *International Journal of Biological Macromolecules*, *135*, 668–676.
- A. O. A. C. (2000). Methods of analysis of AOAC International. AOAC International, Maryland, USA.

- AOCS. (1998). AOCS Official Method Cd 8-53 peroxide value-acetic acid-chloroform method. Official methods and recommended practices of the AOCS.
- Asaduzzaman, A. K. M., Getachew, A. T., Cho, Y. J., Park, J. S., Haq, M., & Chun, B. S. (2020). Characterization of pepsin-solubilised collagen recovered from mackerel (*Scomber japonicus*) bone and skin using subcritical water hydrolysis. *International journal of biological macromolecules*, *148*, 1290–1297.
- Belwal, T., Dhyani, P., Bhatt, I. D., Rawal, R. S., & Pande, V. (2016). Optimization extraction conditions for improving phenolic content and antioxidant activity in Berberis asiatica fruits using response surface methodology (RSM). *Food chemistry*, *207*, 115–124.
- Chamika, W. A. S., Ho, T. C., Roy, V. C., Kiddane, A. T., Park, J. S., Kim, G. D., & Chun, B. S. (2021). In vitro characterization of bioactive compounds extracted from sea urchin (*Stomopneustes variolaris*) using green and conventional techniques. *Food Chemistry*, *361*, 129866.
- Chang, K., Jiang, W., & Liu, J. (2022). Effect of subcritical water treatment on the structure and foaming properties of egg white protein. *Food Hydrocolloids*, *124*, 107241.
- Cho, Y. J., Haq, M., Park, J. S., Lee, H. J., & Chun, B. S. (2019). Physicochemical and biofunctional properties of shrimp (*Penaeus japonicus*) hydrolysates obtained from hot-compressed water treatment. *The Journal of Supercritical Fluids*, *147*, 322–328.
- Chun, B. S., Lee, S. C., Ho, T. C., Micomyiza, J. B., Park, J. S., Nkurunziza, D., & Lee, H. J. (2022). Subcritical Water Hydrolysis of Comb Pen Shell (*Atrina pectinata*) Edible Parts to Produce High-Value Amino Acid Products. *Marine Drugs*, *20*(6), 357.

- Clifford, A. A., & Williams, J. R. (2000). *Introduction to supercritical fluids and their applications* (pp. 1–16). Humana Press.
- Collette, B. B., & Nauen, C. E. (1983). *Scombrids of the world: An annotated and illustrated catalogue of tunas, mackerels, bonitos, and related species known to date*, Vol. 2, Rome: United Nations development programme Food and Agriculture Organization of the United Nations.
- Colombo, M. L. (2010). An update on vitamin E, tocopherol and tocotrienol—perspectives. *Molecules*, *15*(4), 2103–2113.
- Delgado-Andrade, C., Seiquer, I., Haro, A., Castellano, R., & Navarro, M. P. (2010). Development of the Maillard reaction in foods cooked by different techniques. Intake of Maillard-derived compounds. *Food Chemistry*, *122*(1), 145–153.
- Di, Y. U., Chang-Feng, C. H. I., Bin, W. A. N. G., Guo-Fang, D. I. N. G., & Zhong-Rui, L. I. (2014). Characterization of acid- and pepsin-soluble collagens from spines and skulls of skipjack tuna (*Katsuwonus pelamis*). *Chinese Journal of Natural Medicines*, *12*(9), 712–720.
- Doyle, B. B., Bendit, E. G., & Blout, E. R. (1975). Infrared spectroscopy of collagen and collagen-like polypeptides. *Biopolymers: Original Research on Biomolecules*, *14*(5), 937–957.
- Dutta, S., Ray, S., & Nagarajan, K. (2013). Glutamic acid as anticancer agent: An overview. *Saudi Pharmaceutical Journal*, *21*(4), 337–343.
- Franklin, E. C., Haq, M., Roy, V. C., Park, J. S., & Chun, B. S. (2020). Supercritical CO<sub>2</sub> extraction and quality comparison of lipids from Yellowtail fish (*Seriola quinqueradiata*) waste in different conditions. *Journal of Food Processing and Preservation*, *44*(11), e14892.

- García-Moreno, P. J., Horn, A. F., & Jacobsen, C. (2014). Influence of casein-phospholipid combinations as emulsifier on the physical and oxidative stability of fish oil-in-water emulsions. *Journal of Agricultural and Food Chemistry*, *62*(5), 1142–1152.
- Hamadou, A. H., Huang, W. C., Xue, C., & Mao, X. (2020). Comparison of  $\beta$ -carotene loaded marine and egg phospholipids nanoliposomes. *Journal of Food Engineering*, *283*, 110055.
- Hao, G., Cao, W., Li, T., Chen, J., Zhang, J., Weng, W., ... & Ren, H. (2019). Effect of temperature on chemical properties and antioxidant activities of abalone viscera subcritical water extract. *The Journal of Supercritical Fluids*, *147*, 17–23.
- Haq, M., & Chun, B. S. (2018). Characterization of phospholipids extracted from Atlantic salmon by-product using supercritical CO<sub>2</sub> with ethanol as co-solvent. *Journal of Cleaner Production*, *178*, 186–195.
- Haq, M., Suraiya, S., Ahmed, S., & Chun, B. S. (2021). Phospholipids from marine source: Extractions and forthcoming industrial applications. *Journal of Functional Foods*, *80*, 104448.
- Haque, A. R., Park, J. S., Ho, T. C., Roy, V. C., Ali, M. S., Kiddane, A. T., ... & Chun, B. S. (2023). Characterization of oil and amino acids obtained from yellow corvina by-products using subcritical and supercritical fluids. *The Journal of Supercritical Fluids*, *199*, 105970.
- Henderson, J. W., Ricker, R. D., Bidlingmeyer, B. A., & Woodward, C. (2000). Rapid, accurate, sensitive, and reproducible HPLC analysis of amino acids. Amino acid analysis using Zorbax Eclipse-AAA columns and the Agilent, 1–10.
- Je, J. Y., Park, S. Y., Hwang, J. Y., & Ahn, C. B. (2015). Amino acid composition and in vitro antioxidant and cytoprotective activity of

- abalone viscera hydrolysate. *Journal of Functional Foods*, *16*, 94–103.
- Jeong, Y. R., Park, J. S., Nkurunziza, D., Cho, Y. J., & Chun, B. S. (2021). Valorization of blue mussel for the recovery of free amino acids rich products by subcritical water hydrolysis. *The Journal of Supercritical Fluids*, *169*, 105135.
- Jessop, P. G., & Subramaniam, B. (2007). Gas-expanded liquids. *Chemical reviews*, *107*(6), 2666–2694.
- Jung, W. K., Park, P. J., & Kim, S. K. (2003). Purification and characterization of a new lectin from the hard roe of skipjack tuna, *Katsuwonus pelamis*. *The International Journal of Biochemistry & Cell Biology*, *35*(2), 255–265.
- Ishak, I., Hussain, N., Coorey, R., & Abd Ghani, M. (2021). Optimization and characterization of chia seed (*Salvia hispanica L.*) oil extraction using supercritical carbon dioxide. *Journal of CO<sub>2</sub> Utilization*, *45*, 101430.
- Kenneth, L. (2010). *Legal Requirements for Producers Selling Canned Fish into North America*, in: *Fish Canning Handbook*, Hoboken: Wiley–Blackwell.
- Klomklao, S., Benjakul, S., Visessanguan, W., Kishimura, H., & Simpson, B. K. (2007). Purification and characterisation of trypsins from the spleen of skipjack tuna (*Katsuwonus pelamis*). *Food chemistry*, *100*(4), 1580–1589.
- Klomklao, S., & Benjakul, S. (2017). Utilization of tuna processing byproducts: Protein hydrolysate from skipjack tuna (*Katsuwonus pelamis*) viscera. *Journal of Food Processing and Preservation*, *41*(3), e12970.

- Kreps, E. M., Avrova, N. F., Chebotarëva, M. A., Chirkovskaya, E. V., Krasilnikova, V. I., Kruglova, E. E., ... & Zabelinskii, S. A. (1975). Phospholipids and glycolipids in the brain of marine fish. *Comparative Biochemistry and Physiology Part B: Comparative Biochemistry*, *52*(2), 283–292.
- Lee, H. J., Roy, V. C., Ho, T. C., Park, J. S., Jeong, Y. R., Lee, S. C., ... & Chun, B. S. (2021). Amino acid profiles and biopotentiality of hydrolysates obtained from comb penshell (*Atrina pectinata*) viscera using subcritical water hydrolysis. *Marine drugs*, *19*(3), 137.
- Lee, J. H., Ko, M. J., & Chung, M. S. (2018). Subcritical water extraction of bioactive components from red ginseng (*Panax ginseng* CA Meyer). *The Journal of Supercritical Fluids*, *133*, 177–183.
- Lee, S. C., Nkurunziza, D., Kim, S. Y., Surendhiran, D., Singh, A. A., & Chun, B. S. (2022). Supercritical carbon dioxide extraction of squalene rich cod liver oil: Optimization, characterization and functional properties. *The Journal of Supercritical Fluids*, *188*, 105693.
- Lordan, R., Redfern, S., Tsoupras, A., & Zabetakis, I. (2020). Inflammation and cardiovascular disease: are marine phospholipids the answer?. *Food & function*, *11*(4), 2861–2885.
- Lordan, R., Tsoupras, A., & Zabetakis, I. (2017). Phospholipids of animal and marine origin: Structure, function, and anti-inflammatory properties. *Molecules*, *22*(11), 1964.
- Matsumoto, W. M., Skillman, R. A., & Dizon, A. E. (1984). *Synopsis of biological data on skipjack tuna, Katsuwonus pelamis* (No. 136). Washington, DC: National Oceanic and Atmospheric Administration.
- Marik, P. E., & Varon, J. (2009). Omega-3 dietary supplements and the risk of cardiovascular events: a systematic review. *Clinical*

*Cardiology: An International Indexed and Peer-Reviewed Journal for Advances in the Treatment of Cardiovascular Disease*, 32(7), 365–372.

Ministry of Oceans and Fisheries (MOF). (2022a). Ocean Fisheries Statistical Survey. Retrieved from:  
[https://kosis.kr/statHtml/statHtml.do?orgId=146&tblId=DT\\_MLTM\\_5002625&conn\\_path=I2](https://kosis.kr/statHtml/statHtml.do?orgId=146&tblId=DT_MLTM_5002625&conn_path=I2)/Accessed October 23 2023.

Ministry of Oceans and Fisheries (MOF). (2022b). Ocean Fisheries Statistical Survey. Retrieved from:  
[https://kosis.kr/statHtml/statHtml.do?orgId=146&tblId=DT\\_MLTM\\_5002628&conn\\_path=I2](https://kosis.kr/statHtml/statHtml.do?orgId=146&tblId=DT_MLTM_5002628&conn_path=I2)/Accessed October 23 2023.

Mohan, M., Timung, R., Deshavath, N. N., Banerjee, T., Goud, V. V., & Dasu, V. V. (2015). Optimization and hydrolysis of cellulose under subcritical water treatment for the production of total reducing sugars. *RSC advances*, 5(125), 103265–103275.

Mugo, R., Saitoh, S. I., Nihira, A., & Kuroyama, T. (2010). Habitat characteristics of skipjack tuna (*Katsuwonus pelamis*) in the western North Pacific: a remote sensing perspective. *Fisheries Oceanography*, 19(5), 382–396.

Muyonga, J. H., Cole, C. G. B., & Duodu, K. G. (2004). Characterisation of acid soluble collagen from skins of young and adult Nile perch (*Lates niloticus*). *Food chemistry*, 85(1), 81–89.

Park, J. S., Jeong, Y. R., & Chun, B. S. (2019). Physiological activities and bioactive compound from laver (*Pyropia yezoensis*) hydrolysates by using subcritical water hydrolysis. *The Journal of Supercritical Fluids*, 148, 130–136.

- Park, J. S., Roy, V. C., Kim, S. Y., Lee, S. C., & Chun, B. S. (2022). Extraction of edible oils and amino acids from eel by-products using clean compressed solvents: An approach of complete valorization. *Food Chemistry*, *388*, 132949.
- Patil, P. D., Dandamudi, K. P. R., Wang, J., Deng, Q., & Deng, S. (2018). Extraction of bio-oils from algae with supercritical carbon dioxide and co-solvents. *The Journal of Supercritical Fluids*, *135*, 60–68.
- Pike, I. H., & Jackson, A. (2010). Fish oil: production and use now and in the future. *Lipid Technology*, *22*(3), 59–61.
- Plaza, M., Amigo-Benavent, M., Del Castillo, M. D., Ibáñez, E., & Herrero, M. (2010). Facts about the formation of new antioxidants in natural samples after subcritical water extraction. *Food Research International*, *43*(10), 2341–2348.
- Puttikajorn, K., & Benjakul, S. (2020). Simple wet rendering method for extraction of prime quality oil from skipjack tuna eyeballs. *European Journal of Lipid Science and Technology*, *122*(8), 2000077.
- Ramachandraiah, K., Koh, B. B., Davaatseren, M., & Hong, G. P. (2017). Characterization of soy protein hydrolysates produced by varying subcritical water processing temperature. *Innovative Food Science & Emerging Technologies*, *43*, 201–206.
- Roy, V. C., Park, J. S., Ho, T. C., & Chun, B. S. (2022). Lipid indexes and quality evaluation of omega-3 rich oil from the waste of Japanese spanish mackerel extracted by supercritical CO<sub>2</sub>. *Marine Drugs*, *20*(1), 70.
- Sarker, M. Z. I., Selamat, J., Habib, A. S. M. A., Ferdosh, S., Akanda, M. J. H., & Jaffri, J. M. (2012). Optimization of supercritical CO<sub>2</sub> extraction of fish oil from viscera of African catfish (*Clarias*

- gariepinus*). *International journal of molecular sciences*, 13(9), 11312–11322.
- Seo, J. K., Lee, M. J., Jung, H. G., Go, H. J., Kim, Y. J., & Park, N. G. (2014). Antimicrobial function of SH $\beta$ AP, a novel hemoglobin  $\beta$  chain-related antimicrobial peptide, isolated from the liver of skipjack tuna, *Katsuwonus pelamis*. *Fish & shellfish immunology*, 37(1), 173–183.
- Shyni, K., Hema, G. S., Ninan, G., Mathew, S., Joshy, C. G., & Lakshmanan, P. T. (2014). Isolation and characterization of gelatin from the skins of skipjack tuna (*Katsuwonus pelamis*), dog shark (*Scoliodon sorrakowah*), and rohu (*Labeo rohita*). *Food hydrocolloids*, 39, 68–76.
- Shoeb, Z. E., Salama, F. M., & El-Nockrashy, A. S. (1973). Investigations on Fish Oils V. Phospholipid Composition of *Anguilla vulgaris* and *Mugil cephalus*. *Food/Nahrung*, 17(1), 31–40.
- Sila, A., & Bougatef, A. (2016). Antioxidant peptides from marine by-products: Isolation, identification and application in food systems. A review. *Journal of Functional Foods*, 21, 10–26.
- Sook-Kyung, M. (2005). Analysis of total sugar by extraction condition and material to develop the extraction process of ginseng polysaccharide. *Korean Journal of Food Preservation*, 12(4), 367–371.
- Stapleton, P. P., Charles, R. P., Redmond, H. P., & Bouchier-Hayes, D. J. (1997). Taurine and human nutrition. *Clinical nutrition*, 16(3), 103–108.
- Stewart, J. C. M. (1980). Colorimetric determination of phospholipids with ammonium ferrioxalate. *Analytical biochemistry*, 104(1), 10–14.

- Teberikler, L., Koseoglu, S., & Akgerman, A. (2001). Selective extraction of phosphatidylcholine from lecithin by supercritical carbon dioxide/ethanol mixture. *Journal of the American Oil Chemists' Society*, 78, 115–120.
- Turner, C., King, J. W., & Mathiasson, L. (2001). Supercritical fluid extraction and chromatography for fat-soluble vitamin analysis. *Journal of Chromatography A*, 936(1–2), 215–237.
- Underwood, B. A., & Arthur, P. A. U. L. (1996). The contribution of vitamin A to public health. *The FASEB journal*, 10(9), 1040–1048.
- Valentini, K. J., Pickens, C. A., Wiesinger, J. A., & Fenton, J. I. (2018). The effect of fish oil supplementation on brain DHA and EPA content and fatty acid profile in mice. *International journal of food sciences and nutrition*, 69(6), 705–717.
- Villamil, Vaquiro, H., & Solanilla, J. F. (2017). Fish viscera protein hydrolysates: Production, potential applications and functional and bioactive properties. *Food chemistry*, 224, 160–171.
- Wang, Y. M., Li, X. Y., Wang, J., He, Y., Chi, C. F., & Wang, B. (2022). Antioxidant peptides from protein hydrolysate of skipjack tuna milt: Purification, identification, and cytoprotection on H<sub>2</sub>O<sub>2</sub> damaged human umbilical vein endothelial cells. *Process Biochemistry*, 113, 258–269.
- Wheeler, M. D., Ikejema, K., Enomoto, N., Stacklewitz, R. F., Seabra, V., Zhong, Z., ... & Thurman, R. G. (1999). Glycine: a new anti-inflammatory immunonutrient. *Cellular and Molecular Life Sciences CMLS*, 56, 843–856.
- Yao, L., & Jung, S. (2010). <sup>31</sup>P NMR phospholipid profiling of soybean emulsion recovered from aqueous extraction. *Journal of agricultural and food chemistry*, 58(8), 4866–4872.

- Zhang, J., Tao, N., Zhao, Y., Wang, X., & Wang, M. (2019). Comparison of the fatty acid and triglyceride profiles of big eye tuna (*Thunnus obesus*), Atlantic salmon (*Salmo salar*) and bighead carp (*Aristichthys nobilis*) heads. *Molecules*, *24*(21), 3983.
- Zhang, J., Wen, C., Zhang, H., Duan, Y., & Ma, H. (2020). Recent advances in the extraction of bioactive compounds with subcritical water: A review. *Trends in Food Science & Technology*, *95*, 183–195.
- Zhang, L., Zhao, G. X., Zhao, Y. Q., Qiu, Y. T., Chi, C. F., & Wang, B. (2019). Identification and active evaluation of antioxidant peptides from protein hydrolysates of skipjack tuna (*Katsuwonus pelamis*) head. *Antioxidants*, *8*(8), 318.
- Ziero, H. D. D., Ampese, L. C., Sganzerla, W. G., Torres–Mayanga, P. C., Timko, M. T., Mussatto, S. I., & Forster–Carneiro, T. (2022). Subcritical water hydrolysis of poultry feathers for amino acids production. *The Journal of Supercritical Fluids*, *181*, 105492.
- Zuta, P. C., Simpson, B. K., Zhao, X., & Leclerc, L. (2007). The effect of  $\alpha$ -tocopherol on the oxidation of mackerel oil. *Food Chemistry*, *100*(2), 800–807.

## Abstract (In Korean)

### 가다랑어 (*Katsuwonus pelamis*) 부산물의 가치화: 초임계 이산화탄소와 아임계 수 추출을 이용한 지질 및 단백질 회수

신 예 린

국립부경대학교 대학원 식품공학과

#### 요 약

가다랑어 (*Katsuwonus pelamis*)는 수산가공품의 주 원료로 사용되며, 어획 및 가공 과정에서 발생하는 부산물은 원료의 약 50%를 차지한다. 그러나 이러한 부산물의 처리와 폐기는 환경에 부정적인 영향을 미칠 수 있다. 인지질은 친수성 머리 부분과 소수성 꼬리 부분으로 이루어진 양친매성 화합물로, phosphatidylcholine (PC), phosphatidylethanolamine (PE), phosphatidylinositol (PI) 및 lysophosphatidylcholine (LPC) 등을 포함한다. 해양 인지질은 주로 DHA 또는 EPA를 함유한 인지질을 말하며, 이러한  $\omega-3$  지방산은 건강에 다양한 이점을 제공한다. 따라서, 본 연구에서는 청정 기술인 초임계 이산화탄소 및 아임계 수 공정을 활용하여 가다랑어 부산물 (머리, 내장, 껍질)로부터 지질류와 단백질을 회수하고, 이러한 물질들의 물리화학적 및 생리활성 평가를 수행하였다. 초임계 이산화탄소를 이용하여 오일을 추출하였으며 온도 55°C, 압력 30 MPa의 고정된 조건을 사용하였으며, 탈지된 분말을 이용하여 초임계 이산화탄소와 공용매인 에탄올을 사용하여 인지질을 연속적으로 추출하였다. 이때 추출 조건은 온도 40°C, 압력 30 MPa, 이산화탄소 유속 6 mL/min, 공용매 유속은 이산화탄소 유속의 10%로 고정하여 추출 진행되었다. 또한, 탈지분말은 다시 아임계 수 가수분해를 이용하여 단백질을 회수하였으며, 온도 범위 160-240°C에서 비교하였으며, 압력은 4 MPa, 반응시간 15분, 비율 1:50 (w/v)로 고정하여 추출되었다. 가다랑어의 지질 추출에서 껍질에서 얻은 오일이 31.18%  $\pm$  0.59%로 가장 높은 수율을 보였고, 머리와 내장은 각각 14.20%  $\pm$  0.67%와 13.79%  $\pm$  1.05%였다. 인지질의 수득량은 부위별로 다르며, 순 인지질 함량은 머리에서 가장 높게 나타났으며, 각각 3.24%, 2.47%, 1.68%였다. 인지질의  $^{31}\text{P}$  NMR 스펙트럼을 기반으로 정성 및 정량 분석하였으며 주요 클래스로서, PC, PE 및 LPC가 확인되었으며, PC가 주요 클래스 중 70% 이상을 차지했다. 또한, 지질의 주요 지방산으로는 palmitic acid, oleic acid, DHA가 확인되었으며, 이러한 지방산은 오일에서 28.26%, 15.74%, 30.02% 및 인지질에서 7.89%, 15.82%, 19.91%의  $\omega-3$  지방산을 함유하고 있었다. 레티놀은 내장의 오일에서만 1.06  $\pm$  0.02 mg/100g으로 검출되었으며, 토코페롤은 오일과 인지질 모두에 존재하는 주요 비타민으로 오일에서 감마 토코페롤이 29.73  $\pm$  0.13 mg/100g, 17.88  $\pm$  0.02 mg/100g, 76.57  $\pm$  0.84 mg/100g이었고, 인지질에서 25.98  $\pm$  0.12 mg/100g, 18.90  $\pm$  0.11 mg/100g, 19.49  $\pm$  0.09 mg/100g이었다. 열중량 분석 결과를 통해 오일의 단순한 중량 감소를 보여 우수한 열적 안정성을 갖고 있다고 판단하였다. 가다랑어 가수분해물은 온도가 증가함에 따라 추출율이 증가하며 240°C에서 73.17%  $\pm$  0.39%, 90.17%  $\pm$  0.96%, 79.50%  $\pm$  0.12%로 내장 추출물에서 가장 높은 수율을 나타냈다. MRPs 결과를 통해 온도 증가로 마이야르 반응물의 생성이 증가

하는 것을 확인하였다. 총 당함량은 온도가 상승하면서 감소하는 경향을 보였으며, 부위별로  $6.44 \pm 0.22$ 에서  $13.34 \pm 0.67$ ,  $12.81 \pm 0.20$ 에서  $55.19 \pm 0.82$ ,  $6.34 \pm 0.11$ 에서  $13.69 \pm 0.49$  mg glucose/g dried sample으로 다양한 함량을 나타냈다. 환원당은 머리 추출물은  $200^{\circ}\text{C}$ 에서  $8.87 \pm 1.09$  mg glucose/g dried sample, 내장과 껍질 추출물은  $220^{\circ}\text{C}$ 에서  $23.62 \pm 2.04$  mg glucose/g dried sample,  $7.95 \pm 0.43$  mg glucose/g dried sample으로 최대 함량을 나타냈으며, 온도가 증가함에 따라 함량이 감소하는 경향을 보였다. SDS-PAGE를 통해  $160^{\circ}\text{C}$ 에서 부위별로 75 KDa, 35 KDa, 63 KDa이었던 분자량이  $200^{\circ}\text{C}$  이상에서 대부분 저분자화되는 것을 확인했다. 총 단백질 함량은 모든 부위가  $200^{\circ}\text{C}$ 에서  $219.86 \pm 2.26$  mg BSA/g dried sample,  $297.36 \pm 2.17$  mg BSA/g dried sample,  $265.88 \pm 0.85$  mg BSA/g dried sample로 가장 많은 양을 함유되었으며, 온도 상승에 따라 감소하는 경향을 나타냈다. 가장 높은 단백질 함량을 가진  $200^{\circ}\text{C}$  가수분해물의 아미노산 조성을 분석한 결과, 주요 구성아미노산으로는 leucine, glutamic acid, glycine, arginine, alanine 등이 확인되었으며, 주요 유리 아미노산으로는 histidine 및 taurine의 함량이 우세하게 나타났으며 가다랑어 원물과 비교하였을 때 함량의 차이가 발생하였다. 가수분해물의 항산화 활성은 온도가 상승함에 따라 증가하였으며,  $240^{\circ}\text{C}$ 에서  $52.21 \pm 1.05$  mg Trolox/g dried sample,  $80.30 \pm 1.70$  mg Trolox/g dried sample,  $68.28 \pm 7.19$  mg Trolox/g dried sample로 가장 높은 활성을 나타냈다. 항당뇨 활성도 동일하게 온도가 상승함에 따라 증가하였으며 가장 활성이 높았던  $240^{\circ}\text{C}$  가수분해물의  $\alpha$ -glucosidase 억제활성의  $\text{IC}_{50}$  결과, 각각  $6.38 \pm 0.09$  mg/ml,  $2.08 \pm 0.17$  mg/ml,  $5.18 \pm 0.14$  mg/ml으로 내장 추출물이 다른 부위에 비해 가장 높은 활성을 나타냈다. 항염증 활성 역시  $240^{\circ}\text{C}$ 에서 최대활성을 나타내었으며 내장 추출물에서 가장 높은 활성을 나타냈다. 따라서, 본 연구의 결과를 통해 가다랑어는 식품 및 제약 분야에서 활용할 수 있는 유망한 원료로 판단되며, 초임계 이산화탄소 및 아임계 수 추출을 적용함으로써 향후 연구 및 산업에서 선택적으로 활용할 수 있는 중요한 기초자료로 활용될 수 있다.

